Champs-sur-Marne, France

Internship Study Report

3rd year of the Engineering at Indian Institute of Technology, Indore, India

Vibrational study of concrete beams damaged by an internal swelling reaction

Author: **Kumari Sunita**

Internship dates: **May 15 to August 7, 2024**

EMGCU Director: **Renaud-Pierre MARTIN**

Research Supervisors: **Le Hung TRAN**

Silvia IENTILE

Acknowledgment

I would like to express my heartfelt gratitude to my internship supervisor Mr. Le Hung TRAN and Ms. Silvia IENTILE, for the invaluable opportunity to participate and learn in the research under your guidance. Your mentorship and support have been instrumental in my professional growth and learning experience.

Additionally, I extend my sincere thanks to the Director of the University Gustave Eiffel, Mr. Gills ROUSSEL and the Director of the EMGCU Laboratory Mr. Renaud-Pierre MARTIN for their unwavering support and for providing an enriching environment that fostered my development. All the people in the EMGCU laboratory are helpful.

I would like to show my gratitude to Ms. Franziska SCHMIDT, Ms. Fadila GEDJATI and to all other persons, Ms. Célia KHETIB, Ms. Midula ALAM, Mr. Sefatullah MOHAMMADI in the laboratory for each and every support during the internship. The experience has been truly transformative, and I am profoundly grateful for the chance to be a part of such a remarkable team.

I would also like to thanks Director of Ecole des Ingenieurs de la Ville de Paris (EIVP), Mr. Franck JUNG, Ms. Anne LEBAS-SINGNORA, in charge of International Relation from EIVP Institute, with which Indian Institute of Technology, Indore, India has an MoU signed, because of which this internship was possible. She has been very supportive from the starting of the conversation.

Also, my sincere thanks to the Director of Indian Institute of Technology, Indore, Dr. Suhas Joshi, Dean of International Relation with the whole team of International Relation of IIT Indore, for doing all the necessaries and documentation for this internship to make it happen. My deepest gratitude to my professor I.A Palani and to all the members of the laboratory of Instrumental and Control System of IIT Indore for all the support and confidence. Thank you for being my strength.

Abstract

This report presents the research conducted during an internship at the University Gustave Eiffel, in Marne-la-Vallée, specifically at the Expérimentation et Modélisation pour le Génie Civil et Urbain (EMGCU) laboratory, from May 15 to August 7, 2024.

I am a 3rd year bachelor student in Mechanical Engineering at Indian Institute of Technology, Indore, India. In IIT Indore, I have participated in many projects as well as in some research work under prof. I.A Palani in Instrumentation and Control system laboratory since 2022. I have worked on interdisciplinary domain which has always given a chance to know more, learn a lot. This has always encouraged me to search for new dynamic opportunities where I can enhance my skills and work more.

This internship was a good combination of discovering new things, learning and implementing what I had learnt till now. It built me professionally and personally which would help me ahead in life. This experience would support me in my career forward.

This research aimed to analyze the vibrational characteristics of the beams, identifying key parameters that influence their dynamic response Both experimental and theoretical methods were employed, with concrete beam samples undergoing accelerated and natural aging processes before vibrational analysis. The experimental setup included a series of wireless accelerometers and data acquisition systems to measure the vibrational frequencies.

For the theoretical analysis, we used the Euler Bernoulli theory and the Timoshenko theory to comprehend the natural frequencies. The data are taken from the experimentation were analyzed in the software "MATLAB", time domain graph and its frequency domain graph using Fast Fourier Transform has been plotted to get the first natural frequency of the beams. We also did the Numerical Simulation of the beam using Finite Element Method in MATLAB. Then we compared the experimental and the theoretical results with the Numerical results regarding the first natural frequency of the beam.

Key words: **Euler Bernoulli theory, Timoshenko beam theory, MATLAB, Fast Fourier Transform (FFT), Finite Element Method, Experimental Analysis**.

Université Gustave Eiffel • Campus de Marne-la-Vallée
5, Boulevard Descartes • Champs-sur-Marne • 77454 Marne-la-Vallée CEDEX 2• France

Table of content

Université Gustave Eiffel • Campus de Marne-la-Vallée
5, Boulevard Descartes • Champs-sur-Marne • 77454 Marne-la-Vallée CEDEX 2• France

Université Gustave Eiffel • Campus de Marne-la-Vallée
5, Boulevard Descartes • Champs-sur-Marne • 77454 Marne-la-Vallée CEDEX 2• France

List of figures

Université Gustave Eiffel • Campus de Marne-la-Vallée
5, Boulevard Descartes • Champs-sur-Marne • 77454 Marne-la-Vallée CEDEX 2• France

List of Tables

Université Gustave Eiffel • Campus de Marne-la-Vallée
5, Boulevard Descartes • Champs-sur-Marne • 77454 Marne-la-Vallée CEDEX 2• France

1 Introduction

The Internship aims a vibration study of concrete beams damaged by an Internal swelling reaction; the work is to investigate the influence of Delayed Ettringite Formation (DEF) with concrete degradation at the structural scale.

Concrete is a mixture of cement, coarse and fine aggregates of stones, sand and water, also sometimes chemicals are added to set its properties. Concrete is the most widely used materials globally for its strength and durability. The degradation of concrete arises from the three main factors: mechanical (overloads, fatigue), physical (impacts, abrasion, cycles), and chemical (steel corrosion, dissolution of the cement matrix, biodeterioration). Among the chemical factor, Internal swelling reactions (ISR), DEF and Alkali Reacted Reaction (ARR) are the two pathologies which can create expansion, cracking and degradation to its mechanical properties.

Delayed Ettringite Formation (DEF) is a chemical process in concrete that can lead to significant deterioration, particularly in structural elements like beams. DEF occurs when ettringite, a normal byproduct of cement hydration, forms later within the hardened concrete rather than during the initial curing phase. This delayed formation typically happens if the concrete is subjected to high curing temperatures (above 70°C or 158°F) that inhibit early ettringite formation. Once the concrete cools and moisture is available, ettringite forms and expands, generating internal stress that leads cracking, reduced structural integrity, and increased permeability, making the concrete more susceptible to further chemical attacks.

Alkali-Reacted Reaction (ARR) pathologies, often referred to as Alkali-Silica Reaction (ASR), involve a chemical reaction between the alkali hydroxides in concrete and reactive silica found in some aggregates. This reaction produces a gel that absorbs water and expands, creating internal pressure that leads to cracking. The cracks caused by ASR are typically widespread and map-like, and they can significantly impair the mechanical properties and durability of concrete. ASR pathologies are often exacerbated by high moisture and temperatures.

The beams have been manufactured in the laboratory with different concrete mixes and subjected both to accelerated aging in the laboratory and natural aging in the field. Vibration tests were carried out by exciting a force point on the beam, and its dynamic responses in the vertical direction to the axis of beam were captured using accelerometers which were places in different positions which we can see the schematic diagram of the beam in the figure 3.
These measurements are used to obtain the natural frequencies of the beams, which characterize their condition on a structural scale. The work is to analyze the measured signals to obtain the 1st natural frequency of the beam and verify with the Numerical Results, Theoretical Results and the Experimental Results.

Université Gustave Eiffel • Campus de Marne-la-Vallée
5, Boulevard Descartes • Champs-sur-Marne • 77454 Marne-la-Vallée CEDEX 2• France

2 Theoretical Study

2.1 Euler Bernoulli Beam Theory

For structural engineering and mechanics, the fundamental beam theory that is used is the Euler Bernoulli beam theory. It assumes that the material of the beam is linearly elastic and that deformations are small, ensuring that plane sections remain plane and perpendicular to the neutral axis even after bending. The theory's fundamental equations relate bending moments, shear forces, and distributed loads to the beam's deflection and slope, allowing us to predict how beams will respond to external forces.

Let's see a figure of a simply supported beam which follows Euler Bernoulli beam theory which shows that the plane section remains plane.

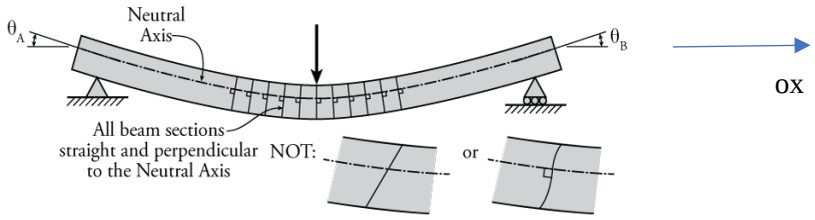

FIGURE 1 EULER BERNOULLI BEAM [1]

It describes the relationship between the bending of a beam and the applied loads in the cartesian coordinates (Oxyz).

$$\frac{\partial^2}{\partial x^2}\left(EI\,\frac{\partial^2 u}{\partial x^2}\right) = q(x,t) \qquad \text{(Eq.1)}$$

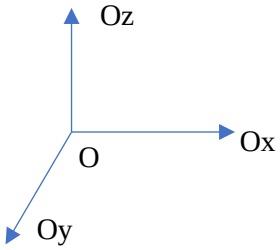

where,

M is bending moment;

E is the Youngs Modulus of elasticity;

I is the moment of inertia of the beam's cross-section about the neutral axis;

$u(x,t)$ is the deflection of the beam in the Oz direction;

$q(x,t)$ is the load per unit length;

x is the position along the beam's length in the Ox direction;

Some key equations,

1. $\theta = \frac{\partial u}{\partial x}$; θ is the slope of the beam
2. $a = \frac{\partial^2 u}{\partial^2 t}$; a is the acceleration
3. $M = EI\,\frac{\partial^2 u}{\partial x^2}$

Université Gustave Eiffel • Campus de Marne-la-Vallée
5, Boulevard Descartes • Champs-sur-Marne • 77454 Marne-la-Vallée CEDEX 2• France

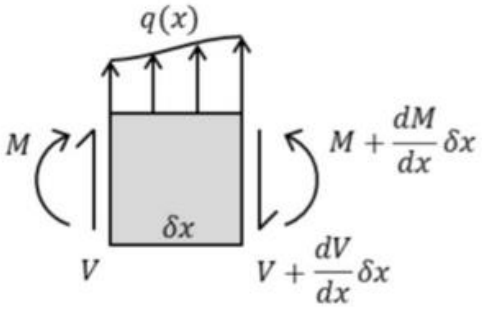

FIGURE 2 FREE BODY DIAGRAM OF A BEAM ELEMENT

Consider a beam element shown in Figure 2 for which $u(x,t)$ is the transverse displacement for a beam and $q(x)$ is the force per unit length along the lateral direction. In the free body diagram of the beam element of the length δx where $V(x,t)$ and $M(x,t)$ are the shear force and bending moment respectively, from the part of the beam on the left of the element. Similarly, $V(x,t) + dV(x,t)$ and $M(x,t) + dM(x,t)$ are the shear force and the bending moment respectively on the part of the beam on the right side of the element.

If we solve the shear force equilibrium equation,

$$V + qdx - (V + dV) = 0 \quad \text{(Eq. 2)}$$

which gives the relation between shear force and load per unit length, $\frac{\partial V}{\partial x} = q$. Similarly, the moment equilibrium equation that is,

$$M + Vdx + qdx\left(\frac{dx}{2}\right) - (M + dM) = 0 \quad \text{(Eq. 3)}$$

we find that $\frac{\partial M(x,t)}{\partial x} = V(x,t)$ or $\frac{\partial^2 M(x,t)}{\partial x^2} = q(x,t)$

Applying Newton's second law of motion to the beam element,

$$\overrightarrow{dF} = dm \,.\, \vec{a} \quad \text{(Eq. 4)}$$

By projecting on the Ox direction of the beam, we have

$$-(\mathrm{v} + \mathrm{dV}) + \mathrm{q} + \mathrm{V} = dm \,.\, a \quad \text{(Eq. 5)}$$

$$-\mathrm{dV} = (\rho \times A)dx\left(\frac{\partial^2 u}{\partial t^2}\right) \quad \text{(Eq. 6)}$$

$$-\frac{\partial^2 M}{\partial x^2} = \rho \times A\left(\frac{\partial^2 u}{\partial t^2}\right) \quad \text{(Eq. 7)}$$

Since there is no external force, q = 0 which means we can deduce the following result:

$$\left(\frac{EI}{\rho A}\right)\frac{\partial^4 u}{\partial x^4} = -\frac{\partial^2 u}{\partial t^2} \quad \text{(Eq.8)}$$

By solving the 4th linear order differential equation, we suppose that the solution would be:

$$u(x,t) = H(x) \,.e^{i\omega_{EB}t} \quad \text{(Eq.9)}$$

where, $H(x)$ is the equation of the mode shape of the beam where the expression is:

Université Gustave Eiffel • Campus de Marne-la-Vallée
5, Boulevard Descartes • Champs-sur-Marne • 77454 Marne-la-Vallée CEDEX 2• France

$$H(x) = [A\sin\gamma x + B\cos\gamma x + C\sinh\gamma x + D\ \cosh\gamma x] \quad \text{(Eq.10)}$$

with,

$$\gamma^4 = \frac{{\omega_{EB}}^2 \rho A}{EI} \quad \text{(Eq.11)}$$

where ω_{EB} is the angular frequency of the Euler Bernoulli's beam theory. Therefore, we get the general equation of beam deflection as follows:

$$u(x,t) = e^{i\omega_{EB}t}[A\sin\gamma x + B\cos\gamma x + C\sinh\gamma x + D\ \cosh\gamma x] \quad \text{(Eq.12)}$$

The 1st, 2nd, 3rd and 4th derivative of aforementioned equation with respect to x are expressed as follows:

$$\begin{cases} u'(x,t) = \gamma \times e^{i\omega_{EB}t}[A\cos\gamma x - B\sin\gamma x + C\cosh\gamma x + D\ \sinh\gamma x] \\ u''(x,t) = \gamma^2 \times e^{i\omega_{EB}t}[-A\sin\gamma x - B\cos\gamma x + C\cosh\gamma x + D\ \sinh\gamma x] \\ u'''(x,t) = \gamma^3 \times e^{i\omega_{EB}t}[-A\cos\gamma x + B\sin\gamma x + C\cosh\gamma x + D\ \sinh\gamma x] \\ u''''(x,t) = \gamma^4 \times e^{i\omega_{EB}t}[A\sin\gamma x + B\cos\gamma x + C\sinh\gamma x + D\ \cosh\gamma x] \end{cases} \quad \text{(Eq. 13)}$$

The 1st, 2nd derivative of $u(x,t)$ with respect to the time t are as follows respectively:

$$\dot{u} = \frac{\partial u}{\partial t} = (i\omega_{EB})H(x).e^{i\omega_{EB}t} \quad \text{(Eq.14)}$$

$$\ddot{u} = \frac{\partial^2 u}{\partial t^2} = -\omega_{EB}^2 H(x).e^{i\omega_{EB}t} \quad \text{(Eq.15)}$$

By replacing the Eq.13 and Eq.14 in Eq.1, we have the following result:

$$\gamma^4 \times e^{i\omega_{EB}t}H(x) - \frac{\omega_{EB}^2 \rho A}{EI}\ H(x).e^{i\omega_{EB}t} = 0$$

Or,

$$\gamma^4.H(x) - \frac{\omega_{EB}^2 \rho A}{EI}\ H(x).e^{i\omega_{EB}t} = 0$$

The Eq.11 will be used in the later part for calculating the first natural frequency.

Now, for solving the deflection equation $u(x,t)$, we need to the boundary conditions.

In this case of simply supported beam, we assume at the starting and the end of the beam will have no deflection, because of the support present, so we can get the following conditions

- At $x = 0$: there is no displacement, therefore:

$$u(0,t) = 0 \quad \text{(Eq.16)}$$

- Likewise, at $x = L$ we have:

$$u(L,t) = 0 \quad \text{(Eq.17)}$$

And also, there are no moments at starting and ending position (the beam is free to rotate), which means the bending moment at these points is zero (the second derivative of y is 0), which gives

- At $x = 0$: $M(0,t) = 0$:

$$u''(0,t) = 0 \quad \text{(Eq.18)}$$

Université Gustave Eiffel • Campus de Marne-la-Vallée
5, Boulevard Descartes • Champs-sur-Marne • 77454 Marne-la-Vallée CEDEX 2• France

- At $x = L$: $M(L,t) = 0$:

$$u''(L,t) = 0 \quad \text{(Eq.19)}$$

Now, if we solve for the equation of $u(x,t)$ by using the boundary conditions Eq.16, we have:

$$e^{i\omega_{EB}t}[A\ \sin\gamma.0 + B\ \cos\gamma.0 + C\ \sinh\gamma.0 + D\ \cosh\gamma.0] = 0 \quad \text{(Eq.20)}$$

which gives:

$$B + D = 0 \quad \text{(Eq.21)}$$

by solving Eq.18, we get the following result:

$$\gamma^2 \times e^{i\omega_{EB}t}[-A\sin\gamma.0 - B\cos\gamma.0 + C\cosh\gamma.0 + D\ \sinh\gamma.0] = 0 \quad \text{(Eq.22)}$$

which gives,

$$-B + D = 0 \quad \text{(Eq.23)}$$

If we solve the above equations, Eq.21 and Eq.23, we find that both B and D turns out to be zero. And to solve for other two coefficients we will have to use another boundary conditions that is Eq 17 and Eq.19.

Now,

$$e^{i\omega_{EB}t}[-A\sin\gamma.L - B\cos\gamma.L + C\cosh\gamma.L + D\ \sinh\gamma.L] = 0 \quad \text{(Eq.24)}$$

$$\gamma^2 \times e^{i\omega_{EB}t}[-A\sin\gamma.L - B\cos\gamma.L + C\cosh\gamma.L + D\ \sinh\gamma.L] = 0 \quad \text{(Eq.25)}$$

We can also represent the Eq.24 and Eq.25 it in the form of matrix and solve it as follows:

$$\begin{bmatrix} \sin\gamma L & \sinh\gamma L \\ -\sin\gamma L & \sinh\gamma L \end{bmatrix}\begin{bmatrix} A \\ C \end{bmatrix} = \begin{bmatrix} 0 \\ 0 \end{bmatrix} \quad \text{(Eq.26)}$$

For a nontrivial solution, we know the determinant of the matrix should be zero.

$$\det\begin{bmatrix} \sin\gamma L & \sinh\gamma L \\ -\sin\gamma L & \sinh\gamma L \end{bmatrix} = 0 \quad \text{(Eq.27)}$$

Or,

$$2(\sin\gamma L)(\sinh\gamma \mathrm{L}) = 0 \quad \text{(Eq.28)}$$

It should be noted that, $\sinh\gamma \mathrm{L} \neq 0$, which implies that $C = 0$;

Therefore, we can say $\sin\gamma L = 0$ and for the characteristic equation, we have B, C and D equals to 0 and hence can be written as:

$$u(x,t) = A\ \sin\gamma x\ .\ e^{i\omega_{EB}t} \quad \text{(Eq.29)}$$

So, $\gamma \mathrm{L} = n\pi$ with $n \in N^*$

$\gamma = \frac{\mathrm{n}\,\pi}{L}$, the same as before mentioned in Eq.11

The angular frequency comes out to be:

Université Gustave Eiffel • Campus de Marne-la-Vallée
5, Boulevard Descartes • Champs-sur-Marne • 77454 Marne-la-Vallée CEDEX 2• France

$$\omega_{EB} = \frac{n^2\pi^2}{L^2}\sqrt{\frac{EI}{\rho A}} \qquad \text{(Eq.30)}$$

2.2 Frequency using Timoshenko Beam Theory:

When we work with Euler Bernoulli theory, one of the limitations is, it can be applicable if the ratio of length of the beam is significantly larger than the height of the beam. And if $\frac{l}{h} < 10$ then we use the Timoshenko Beam and for the simply supported beam, when we saw the values of length of beam and its height (reference Table 4), we found that $\frac{l}{h}$ =6.06 which is less than 10. It is important to consider Timoshenko beam theory formulation for analysis of first natural frequency of beam in this case.

The Formula is as follows:

$$\omega_{TM}^2 = \frac{\omega_{EB}^2 L^2}{2j^2\pi^2 r^2}\left\{1 + \frac{c_2^2}{{c_1}^2} + \frac{c_2^2}{{c_1}^2}\left(\frac{L^2}{j^2\pi^2 r^2}\right) - \left[\sqrt{1 + \frac{c_2^2}{{c_1}^2} + \frac{c_2^2}{{c_1}^2}\left(\frac{L^2}{j^2\pi^2 r^2}\right)^2 - 4\left(\frac{c_2^2}{{c_1}^2}\right)}\right]\right\} \qquad \text{(Eq.31)}$$

Where j is the number of natural mode and the other parameters are detailed as shown in the following table:

Notation	Parameters
ω_{TM}	Angular frequency using Timoshenko theory;
ω_{EB}	Angular frequency using Euler Bernoulli theory;
$c_2 = \frac{\kappa \times G}{\rho}$	Velocity of propagation of transverse wave;
κ	Constant dependent on the shape of the section with $\left(\kappa = \frac{2}{3}\right)$ for rectangular shape of cross section of the beam;
$G = \frac{E}{2(1+\nu)}$	Modulus of elasticity in shear;
ν	Poisson's ratio;
ρ	Mass density of the beam;
$c_1 = \frac{E}{\rho}$	Velocity of propagation of longitudinal wave;
$r^2 = \frac{I}{A}$	Radius of gyration for the beam;
I	Second moment of Inertia of the beam;
A	Cross sectional area of the beam.

TABLE 1 PARAMETERS IN TIMOSHENKO THEORY

2.3 Numerical Application

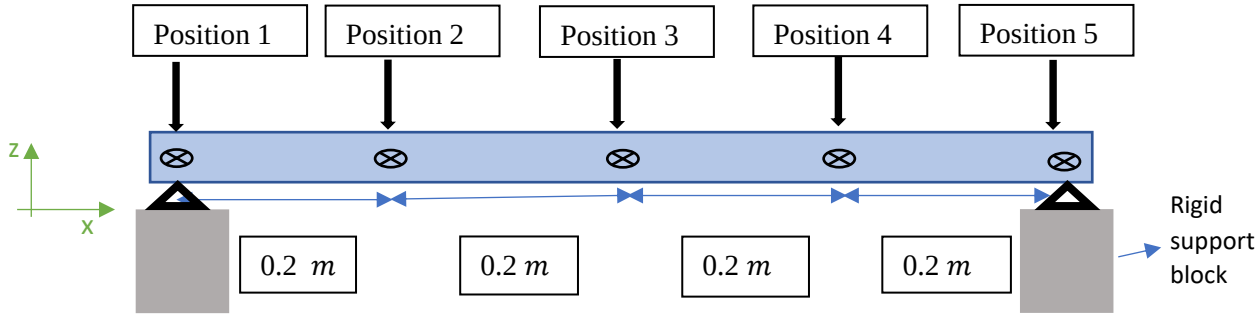

Université Gustave Eiffel • Campus de Marne-la-Vallée
5, Boulevard Descartes • Champs-sur-Marne • 77454 Marne-la-Vallée CEDEX 2• France

FIGURE 3 SCHEMATIC DIAGRAM OF THE BEAM WITH THE 5 ACCELEROMETER POSITION

FIGURE 4 A) SIDE VIEW OF BEAM B) BEAM CROSS SECTION

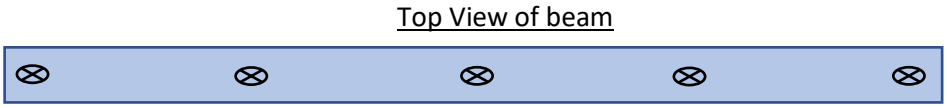

FIGURE 5 TOP VIEW OF THE BEAM

In the above Figure 3, the schematic diagram of the beam is shown with 5 accelerometer and its mentioned position which is used in the experimentation.

In the Table 2, we have the information about the beams we used and the condition under which it has been kept.

Beam	Name of the beam	Young's Modulus (GPa)	Poisson's ratio	Conditions under which it has been kept
1st	VL_R1FNTT_Vib-COBE_L_ent	41.4	0.19	Accelerated aging process with a cut in the middle
2nd	VL_R1FNTT_Vib-COBE_L	41.4	0.19	Accelerated aging process
3rd	VL_R1F_Vib-COBE_L	37.3	0.173	Accelerated aging process
4th	VN_R1F_NTT_VIB-COBE-VN	41.4	0.19	Natural aging process
5th	VN_R1F_VIB-COBE-VN	37.3	0.173	Natural aging process

TABLE 2 INFORMATION OF THE BEAM

FIGURE 6 BEAM WITH A CUT AT THE MIDDLE

Université Gustave Eiffel • Campus de Marne-la-Vallée
5, Boulevard Descartes • Champs-sur-Marne • 77454 Marne-la-Vallée CEDEX 2• France

FIGURE 7 BEAM WITHOUT A CUT

Above, in Eq.30 and Eq.31 we saw the formulation for the different theories for the calculation of the natural frequency of the beam, if we solve for the first natural frequency using the values of the parameters shown in the Table 4, we get the results as follows:

Beam Names	1st natural frequency using EB theory f_{EB} (Hz)		1st natural frequency using TM theory f_{TB} (Hz)	
	L=0.8 m	L =1 m	L =0.8 m	L =1 m
First beam VL_R1FNTT_Vib-COBE_L_ent	366.85	252.09	350.92	249.73
Second beam VL_R1FNTT_Vib-COBE_L	366.85	252.09	350.92	249.73
Third beam VL_R1F_Vib-COBE_L	348.26	223.62	333.51	221.87
Forth beam VN_R1F_NTT_VIB-COBE-VN	366.85	252.09	350.92	249.73
Fifth beam VN_R1F_VIB-COBE-VN	348.26	223.62	333.51	221.87

TABLE 3 CALCULATION OF THE FIRST NATURAL FREQUENCY OF ALL BEAMS

We see that from Eq.30,

$$\omega_{EB} = \frac{n^2\pi^2}{L^2}\sqrt{\frac{EI}{\rho A}}$$

In case of Euler Bernoulli theory, the angular frequency depends upon the length of the beam. If the length of the beam increases then the frequency decreases, therefore we have calculated for two different lengths of the beam.

We also calculated the results from Timoshenko beam theory because unlike the Euler-Bernoulli theory, which assumes that cross-sections remain perpendicular to the neutral axis after deformation, the Timoshenko theory allows for a shear strain. This means cross-sections can rotate, and shear deformation is considered, making it more accurate for analyzing dynamic behavior and vibrations of the beam.

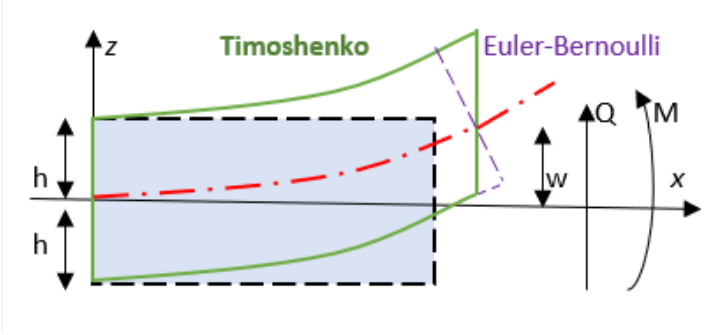

FIGURE 8 COMPARISON BETWEEN EULER-BERNOULLI AND TIMOSHENKO IN SHOWING PLANE OF SHEAR [2]

We can clearly find that the plane of cross-sectional is not perpendicular to the neutral axis and this is because of the shear effect.

Université Gustave Eiffel • Campus de Marne-la-Vallée
5, Boulevard Descartes • Champs-sur-Marne • 77454 Marne-la-Vallée CEDEX 2• France

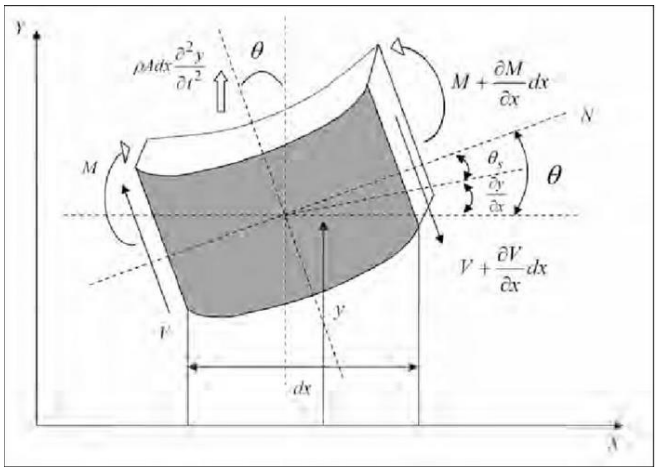

FIGURE 9 FREE BODY DIAGRAM OF TIMOSHENKO BEAM ELEMENT [3]

We can see in the Figure 9 which shows a beam element corresponding to the Timoshenko beam theory.

For beams where the length is comparable to the height, shear deformation and rotational inertia significantly affect the beam's behavior. Timoshenko theory provides a more accurate description than Euler-Bernoulli theory. Therefore, Timoshenko theory is an enhancement of the Euler-Bernoulli beam theory

The deflection of short beams is more accurately predicted by the Timoshenko theory because it accounts for shear deformation, which contributes significantly to the total deflection.

Also, the natural frequencies of short beams are rightly calculated by the Timoshenko theory due to its consideration of shear deformation and rotational inertia. For long beams, the natural frequencies predicted by both theories almost converge.

Université Gustave Eiffel • Campus de Marne-la-Vallée
5, Boulevard Descartes • Champs-sur-Marne • 77454 Marne-la-Vallée CEDEX 2• France

3. Numerical Simulation

3.1 Finite Element Analysis

Finite Element Analysis (FEA) is a computational technique used to predict how objects will respond to external forces, heat, fluid flow, and other physical effects. By dividing a complex structure into smaller, manageable finite elements, FEA approximates the behavior of the structure under various conditions. Each element is analyzed individually using mathematical equations, and then the results are combined to predict the overall behavior of the structure. This method is particularly useful for solving problems involving complex geometries, material properties, and boundary conditions that are difficult to address using analytical methods.

Finite Element Analysis (FEA) for concrete beams is a specialized application of the Finite Element Method (FEM) tailored to analyze and predict the behavior of concrete structures under various loading conditions. Concrete, being a heterogeneous and quasi-brittle material, presents unique challenges in modeling due to its complex stress-strain relationship, cracking behavior, and time-dependent properties like creep and shrinkage. FEM helps address these challenges by discretizing a concrete structure into small elements, applying appropriate material models that capture the non-linear behavior of concrete, and solving the governing equations to predict responses such as stress distribution, crack formation, and deformation under different loading scenarios.

By simulating how concrete structures respond to loads, environmental conditions, and potential defects, engineers can optimize the design for performance and longevity, identify potential failure modes, and make informed decisions about material selection and construction methods. FEM for concrete not only enhances the understanding of structural behavior but also helps in complying with safety standards and reducing the reliance on empirical design approaches, leading to more efficient and innovative structural solutions.

Therefore, we used FEM for the concrete beams prepared in the laboratory, to know the natural frequencies of the two mixtures.

3.2 Simulation with MATLAB

3.2.1 3-D Model in Autodesk

Autodesk Fusion 360 is a versatile cloud-based 3D computer-aided design (CAD), Computer-Aided Manufacturing (CAM), and Computer-Aided Engineering (CAE) tool designed to support the entire product development process. It combines industrial and mechanical design, simulation, collaboration, and machining in a single integrated platform.

We build a 3D geometry and export it in the format of ".stl". It stands for "Stereolithography." The STL file format is widely used in CAD and 3D printing. STL files describe the surface geometry of a three-dimensional object without any representation of color, texture, or other attributes. The STL format uses a series of triangular facets to approximate the shape of an object.

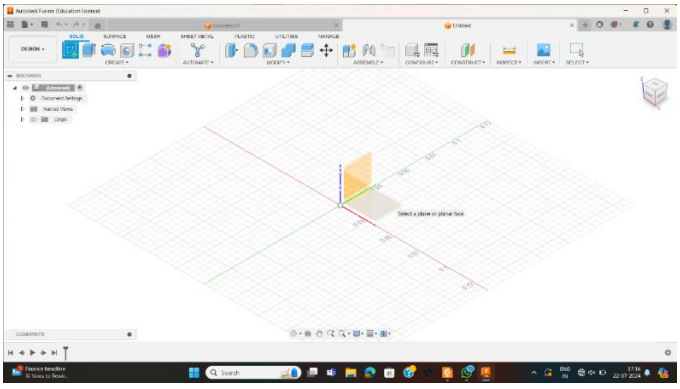

Université Gustave Eiffel • Campus de Marne-la-Vallée
5, Boulevard Descartes • Champs-sur-Marne • 77454 Marne-la-Vallée CEDEX 2• France

FIGURE 10 INTERFACE OF AUTODESK FUSION 360

In Figure 10, the interface of software Autodesk Fusion 360 is shown. We can also perform the 3D geometry modelling in other software like SolidWorks, AutoCAD etc.

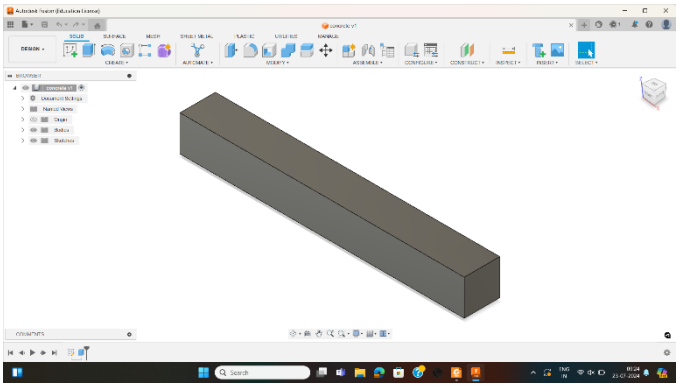

FIGURE 11 3D GEOMETRY MODEL

Figure 11 shows the model made in the Autodesk Fusion 360.

3.2.2 MATLAB programming

To perform FEM in the MATLAB:

- We need to import the 3D geometry that we created in the Autodesk Fusion 360.
- Then we define the structural properties of the concrete beam that we had with us.
- The mesh is automatically generated by MATLAB with using suitable code.
- We also give the boundary conditions to a simply supported beam to the model.

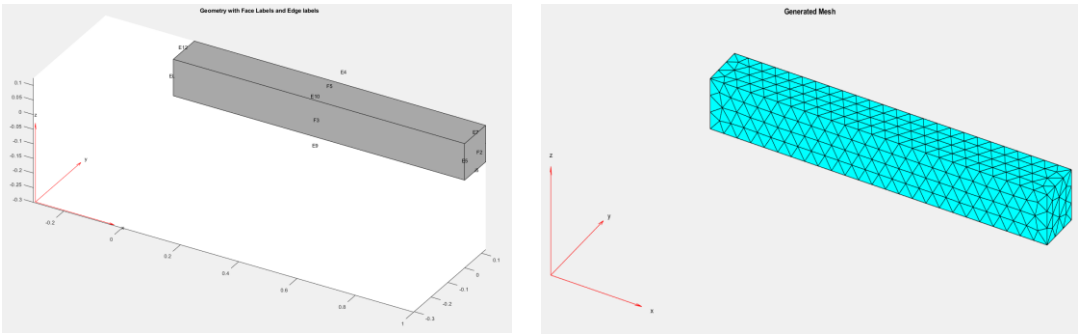

FIGURE 12 A) FACE LABELS AND EDGE LABELS OF THE MODEL B) GENERATED MESH

Figure 12A describes the imported model from Fusion 360 and plotted by MATLAB software, with the face labels and the edge labels mentioned in it, so that to give the boundary conditions of the beam we can identify them. Figure 12B shows the generated mess in the MATLAB.

3.3 Numerical Result by using Finite Elements Method (FEM)

Here is the result from the MATLAB simulation through FEM application. We had two different mixtures of concrete. One is named as RIF and another is RIF_NTT.

Université Gustave Eiffel • Campus de Marne-la-Vallée
5, Boulevard Descartes • Champs-sur-Marne • 77454 Marne-la-Vallée CEDEX 2• France

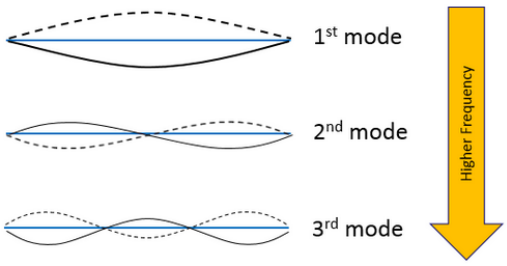

FIGURE 13 MODE SHAPE OF SIMPLY SUPPORTED BEAM [4]

This Figure 13 which shows the mode shape of the simply supported beam. A mode shape is a specific pattern of deformation that a structure or mechanical system undergoes at a particular natural frequency during vibration. When a structure vibrates, it can do so in several different ways, each characterized by a unique distribution of displacements, strains, and stresses throughout the structure. These unique patterns of vibration are called mode shapes. Each mode shape corresponds to a specific natural frequency, which is a frequency at which the structure naturally tends to oscillate in the absence of damping and external forces. In vibration analysis, mode shapes are used to understand how different parts of a structure move relative to each other when vibrating at a natural frequency. This is critical for predicting and mitigating potential resonance, which can lead to excessive vibrations and even structural failure.

The detailed information of the concrete mixtures and the beams that were made from the concrete mixtures, can be found in Page 22 and 23.

- Concrete mixture RIF

The specifications of the beam used in the following result:

Young's Modulus: 41.4 GPa

Poisson's ratio :0.19

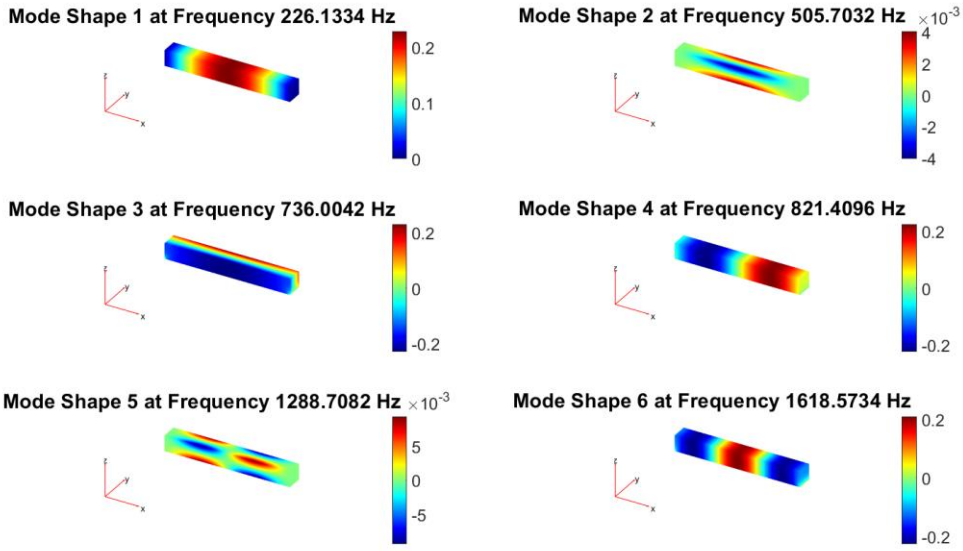

FIGURE 14 NATURAL FREQUENCY OF RIF MIXTURE

The Figure14 shows the first natural frequency to be 226.13 Hz.

Université Gustave Eiffel • Campus de Marne-la-Vallée
5, Boulevard Descartes • Champs-sur-Marne • 77454 Marne-la-Vallée CEDEX 2• France

- Concrete mixture RIF_NTT

The specifications of the beam used in the following result:

Young's Modulus: 37.3 GPa

Poisson's ratio :0.173

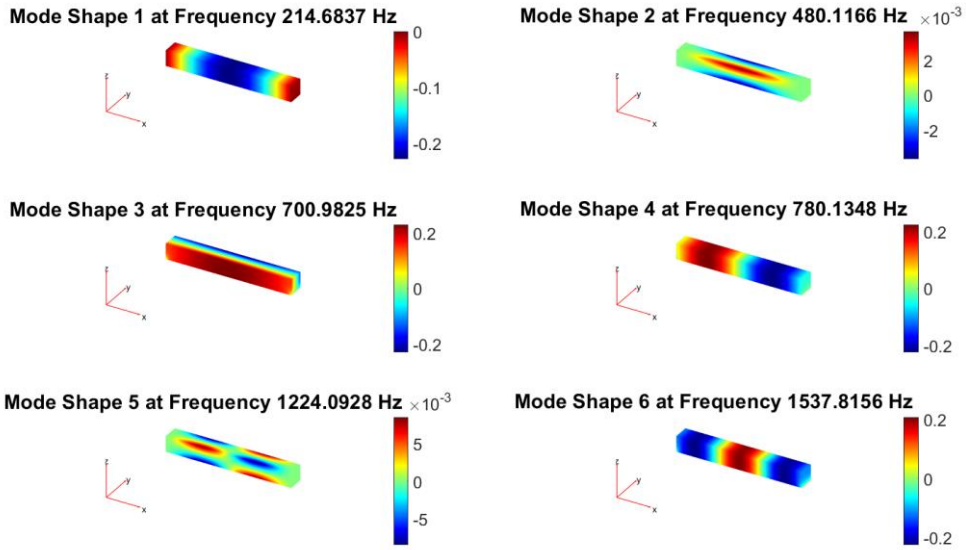

FIGURE 15 NATURAL FREQUENCY OF RIF_NTT MIXTURE

The Figure15 shows the first natural frequency to be 214.68 Hz.

Université Gustave Eiffel • Campus de Marne-la-Vallée
5, Boulevard Descartes • Champs-sur-Marne • 77454 Marne-la-Vallée CEDEX 2• France

4. Experimental Studies of the concrete beams

4.1 Concept

4.1.1 Introduction

A)  B) 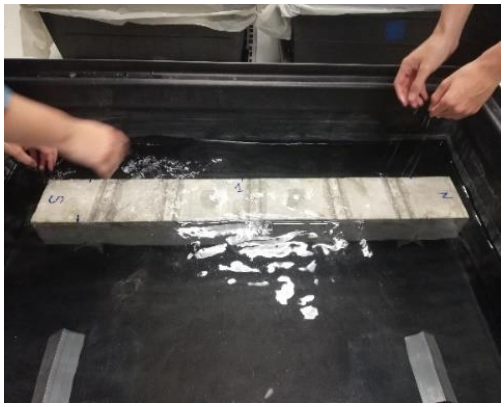

FIGURE 16 A) BEAM WITH FIVE ACCELEROMETER B) BEAM EMERGED IN WATER

C) 

C) BEAM KEPT OUTSIDE

There were two similar kinds of mixture made in the EMGCU laboratory named as RIF and RIF_NTT. In RIF, a chemical named potassium hydroxide was added to the mixture, then it was heated at 81℃ for 3 days under water just after casting was done to trigger the Delayed Ettringite formation (DEF). Two beams were made with this material. One kept inside the laboratory and another outside.

For RIF_NTT material just after the casting was done, it was emerged in water at 20℃. Three beams were made with it, two of them kept inside the laboratory and one outside the laboratory to undergo natural change.

As a result, we have concrete beams which are kept in two different environmental conditions, total there are 5 simply supported beams, 3 among them are kept under accelerated aging process (temperature 20℃ and humidity 60%) shown in Figure 16B and other two are under natural aging process shown in Figure16C. To carry out the experiment, we took the first beam, we placed 5 different accelerometers at certain distance on the beam as shown in the Figure 16A which we call them positions and after that a first testcase 1 is made and data are recorded in all 5 positions and then after couple of minutes second testcase 2 is being made and then again data is recorded. And the similar activity is done for the other beams too.

Université Gustave Eiffel • Campus de Marne-la-Vallée
5, Boulevard Descartes • Champs-sur-Marne • 77454 Marne-la-Vallée CEDEX 2• France

The data is taken at three different time intervals, first batch of data was taken during July 2023 which is considered to be at reference time; t=0, second batch was during September 2023 and thirdly in November 2023.

And recently, June 2024 another batch of experiment was conducted and data has been recorded.

The following study is done on the data collected in July, 2023 this was the time when the beams were newly prepared.

4.1.2 Units and values used in beam analysis

These are the following values for the parameters on which frequency of the beam depends:

Parameter	Values	Units	Notation
Youngs Modulus for the Mixture RIF (first, second and fourth beam)	41.4	GPa	E
Youngs Modulus for the Mixture RIF_NTT (third and fifth beam)	37.3	GPa	E
Mass density	2416	$Kg.m^{-3}$	ρ
Poisson ratio for first, second and fourth beam	0.19	-	ν
Poisson ratio for third and fifth beam	0.173	-	ν
Length of the beam	0.8	m	L
Breadth of the beam	0.125	m	b
Height of the beam	0.125	m	h
Area of cross section	0.0156	m^2	A
Second moment of Inertia	2.0345×10^{-5}	m^4	I

TABLE 4 UNITS AND VALUES OF THE PARAMETERS

4.2 Materials Required for the vibration test

To carry out the vibration test, we used the following equipment:

- **Accelerometer sensor**

A)  B) 

FIGURE 17 A) FIVE DIFFERENT ACCELEROMETER B) INTERNAL IMAGE OF AN ACCELEROMETER

We used the above shown accelerometer sensors for our data acquisition which was wireless to store reading from the beam. Accelerometer sensor were well calibrated by the EMGCU laboratory to handle the experiments properly.

Wireless accelerometer sensors are devices that measure acceleration forces and transmit this data wirelessly to a receiver or a data processing system. The core component of these sensors is a micro-electromechanical system (MEMS) accelerometer, which can convert mechanical motion into an electrical signal. This data is then wirelessly transmitted using communication protocols like Bluetooth, Wi-Fi, etc. enabling real-time monitoring and analysis. One of the primary advantages of wireless accelerometer sensors is their flexibility and ease of installation. Without the constraints of physical

cabling, these sensors can be placed in hard-to-reach or mobile environments, making them ideal for applications in remote monitoring, industrial machinery, automotive systems, etc.

These accelerometer can record the data in 3 axes,in our experiment x direction which corresponds to the axis of beam, y direction and z diection which is the vertical to the axis of the beam.While taking reading, we collected the data in all 3 direction, but in the analysis we worked with the vertical direction displacement that is z direction. These accelerometer works in two different mode; lock mode and transmit mode.

In **Lock mode**, data is stored in the internal memory of the sensors. This mode is particularly useful in applications where continuous monitoring is not necessary, allowing the device to remain dormant and preserve energy until needed.

Transmit mode is crucially for real-time monitoring applications where timely and accurate acceleration data is required**.** Transmit mode is the active state where the wireless accelerometer performs its primary functions of measuring acceleration forces and transmitting this data wirelessly to a receiver. This mode involves continuous data collection and frequent transmission, leading to higher power consumption.

Here, we worked in the Lock mode, as we did not want the real time monitoring, we stored the data in the internal memory and then later we download the csv files from the software, that is mentioned below.

- **Hammer for making an impact on the beam**

A)  B) 

FIGURE 18 A) IMPACTING ON A BEAM DURING THE EXPERIMENT B) HAMMER

We can see in the Figure 18A, which was taken during the experimentation in June 2024 and Figure 18B shows the hammer we used for the impact during our experimentation.

- **System Measurement**

The software used for the data collection is “SensorConnect”, where we set the sampling frequency. Sampling frequency, denotes to the sampling rate, is the number of samples taken per second from a continuous signal to make it discrete. The choice of sampling frequency affects the quality and fidelity of the digital representation of the signal. The Sampling frequency that we used for the experiment is 4096 Hz.

And then we downloaded the data in the form of CSV files, which was used for analyzing the signal in MATLAB software to visualize the time domain graph and frequency domain graph.

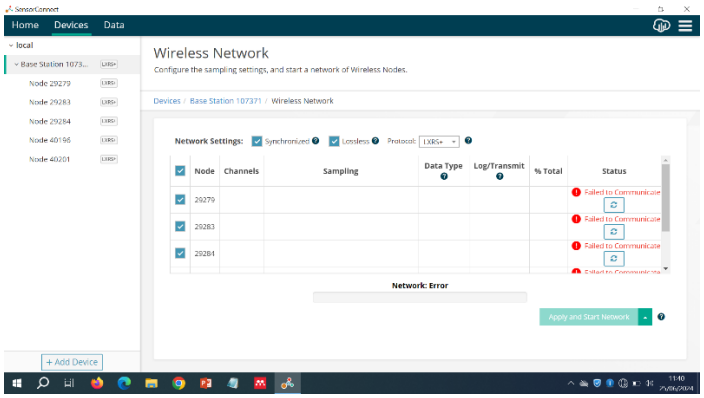

FIGURE 19 INTERFACE OF SOFTWARE SENSORCONNECT

4.3 Visualization of signal of beam

The software which is used to visualized the time domain graph of the reading that were carried out during the experimentation is **MATLAB**.

MATLAB (MATrix LABoratory) is a high-level programming language and interactive environment developed by MathWorks. It is widely used for numerical computing, data analysis, algorithm development, and visualization. MATLAB includes a variety of toolboxes that extend its functionality for specific applications such as signal processing, control systems and more. Used extensively in various fields of engineering, science, and mathematics for research, development, and testing. MathWorks provides comprehensive documentation and user guides.

Now, we have the time domain graphs from the data collected during the experimentation for all the 5 beams.

4.3.1 Time domain graphs for the first beam (VL_R1FNTT_Vib-COBE_L_ent)

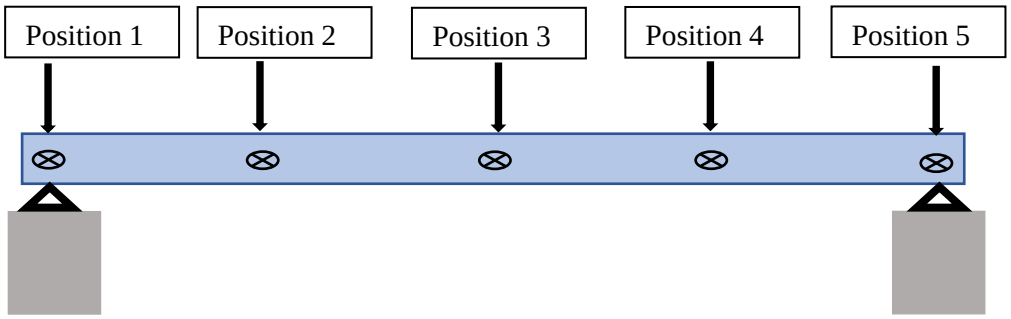

For the below time domain graph, here is the reference of all the positions of the accelerometer shown in the above Figure.

We conducted only two testcases for this first beam, where the signal of testcase 2 do not give the desired output as testcase 1 gives, therefore we have the plot of testcase 1 as follows:

Université Gustave Eiffel • Campus de Marne-la-Vallée
5, Boulevard Descartes • Champs-sur-Marne • 77454 Marne-la-Vallée CEDEX 2• France

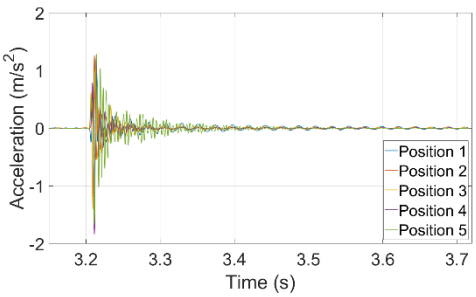

FIGURE 20 BEAM 1 TESTCASE 1

4.3.2 Time domain graphs for the second beam (VL_R1FNTT_Vib-COBE_L)

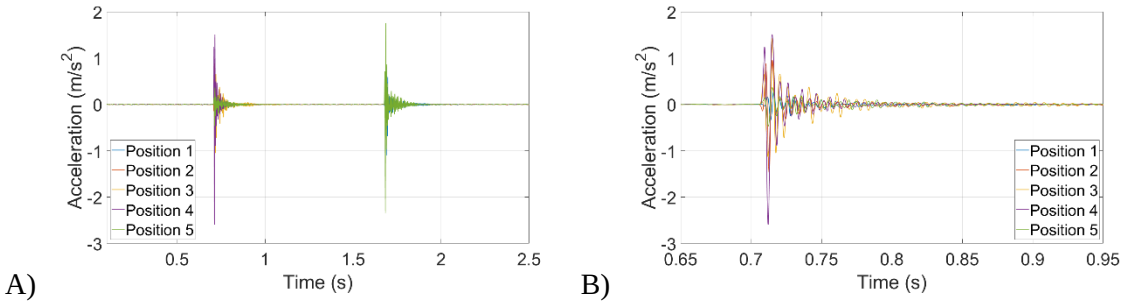

FIGURE 21 A) SECOND BEAM TESTCASE 1 B) HAMMER IMPACT 1

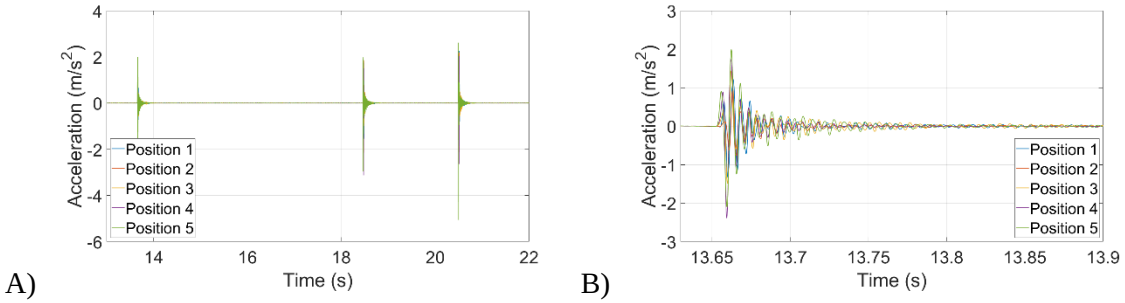

FIGURE 22 A) SECOND BEAM TESTCASE 2 B) HAMMER IMPACT 1

We can see for the second beam in the Figure 21A, from testcase 1 we have 2 hammer impact which shows 2 peaks but in the second hammer impact we have signal from only two position, Figure 21B shows the first hammer impact of it. Figure 22A from the testcase 2 we have 3 hammer impacts that why we have 3 peaks for all the accelerometer position. Figure 22B shows the first hammer impact of it.

4.3.3 Time domain graphs for the third beam (VL_R1F_Vib-COBE_L)

We can see in the Figure 23A, from the testcase 1 we have 3 hammer impacts that why we have 3 peaks for all the accelerometer position and in Figure 24A, from testcase 2 we have 3 hammer impacts.

Figure 23B shows the first hammer impact for testcase1 and Figure 24B shows the first hammer impact for testcase2.

Université Gustave Eiffel • Campus de Marne-la-Vallée
5, Boulevard Descartes • Champs-sur-Marne • 77454 Marne-la-Vallée CEDEX 2• France

A)

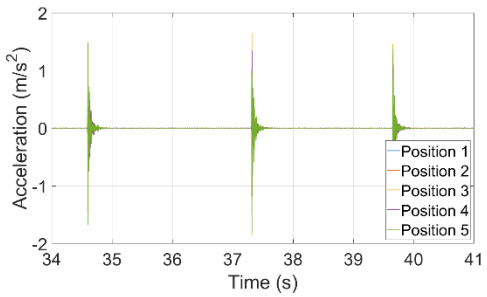

B)

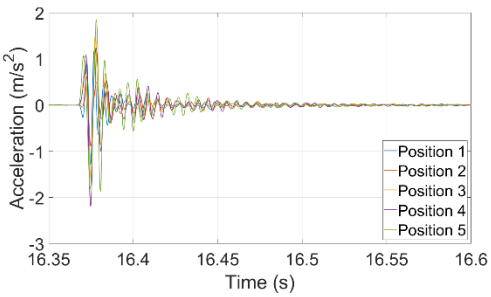

FIGURE 23 A) THIRD BEAM TESTCASE 1 B) HAMMER IMPACT 1

A)

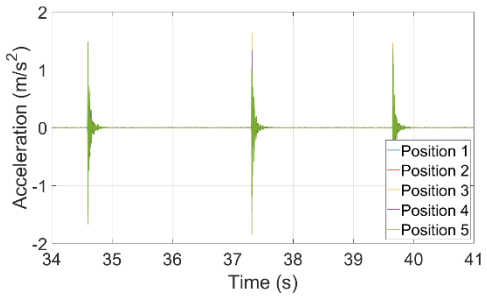

B)

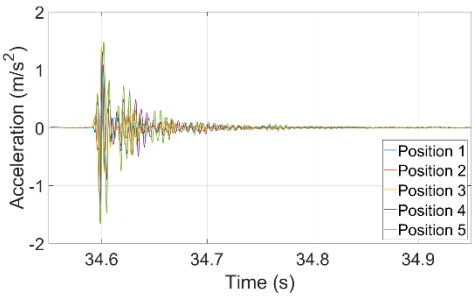

FIGURE 24A) THIRD BEAM TESTCASE 2 B) HAMMER IMPACT 1

4.3.4 Time domain graphs for the fourth beam (VN_R1F_NTT_VIB-COBE-VN)

We can see in the Figure 25A, from the testcase 1 we have 3 hammer impacts showing 3 peaks for all the accelerometer position and in Figure 26A, from testcase 2 we have 3 hammer impacts.

Figure 25B shows the first hammer impact for testcase1 and Figure 26B shows the first hammer impact for testcase2

A)

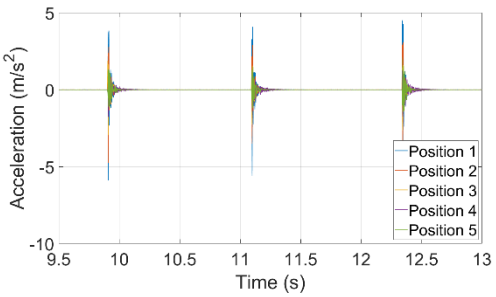

B)

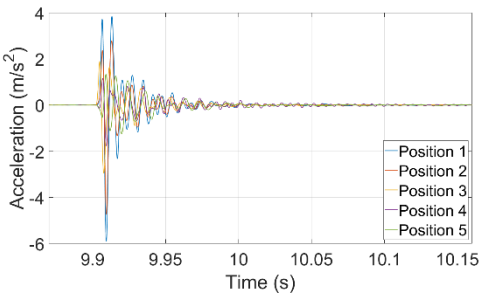

FIGURE 25A) FORTH BEAM TESTCASE 1 B) HAMMER IMPACT 1

Université Gustave Eiffel • Campus de Marne-la-Vallée
5, Boulevard Descartes • Champs-sur-Marne • 77454 Marne-la-Vallée CEDEX 2• France

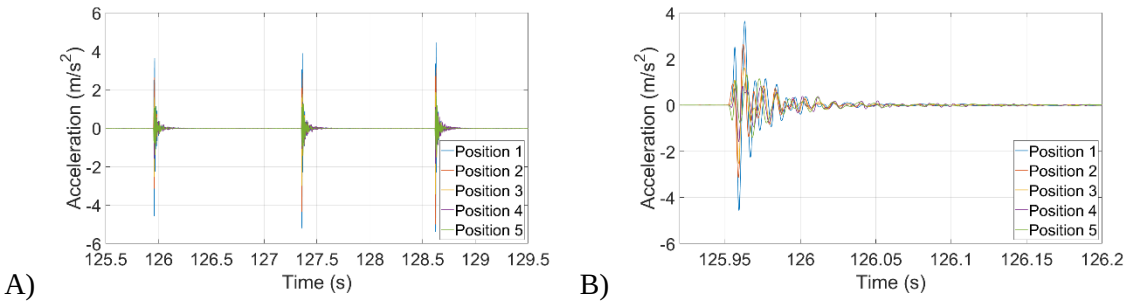

FIGURE 26A) FOURTH BEAM TESTCASE 2 B) HAMMER IMPACT 1

4.3.5 Time domain graphs for the fifth beam (VN_R1F_VIB-COBE-VN)

Similarly, we can see in the Figure 27A, from the testcase 1 we have 3 hammer impacts with 3 peaks for all the accelerometer position and in Figure 28A, from testcase 2 we have 3 hammer impacts.

Figure 27B shows the first hammer impact for testcase1 and Figure 28B shows the first hammer impact for testcase2

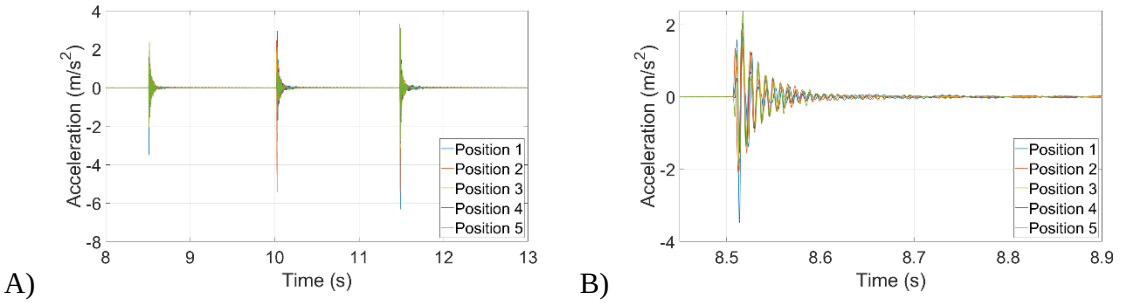

FIGURE 27A) FIFTH BEAM TESTCASE 1 B) HAMMER IMPACT 1

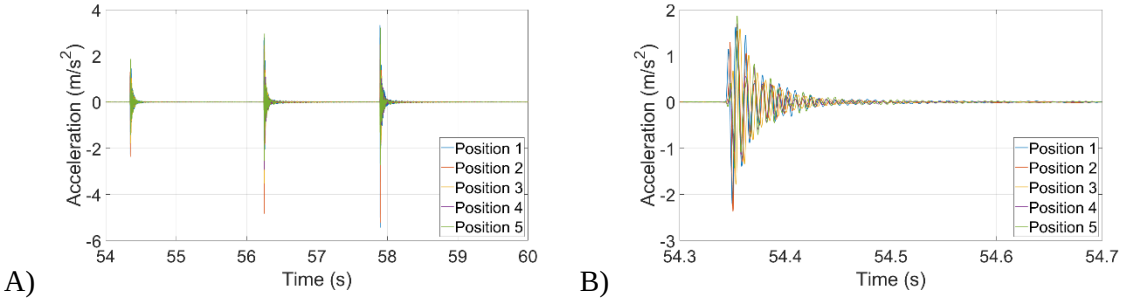

FIGURE 28A) FIFTH BEAM TESTCASE 2 B) HAMMER IMPACT 1

4.4 Analysis of Frequency

For the frequency graph, we did the Fast Fourier transformation in `MATLAB` which is denoted by `fft`.

The Fast Fourier Transform (FFT) in `MATLAB` is a powerful algorithm for computing the Discrete Fourier Transform (DFT) and its inverse, crucial for signal processing, image analysis, and various engineering applications. Using the fft function, `MATLAB` efficiently transforms time-domain signals into their frequency components, allowing for the analysis of signal characteristics such as frequency, amplitude, and phase.

Let's suppose, `Y=fft (X)` computes the discrete Fourier transform (DFT) of X signal using a Fast Fourier Transform (FFT) algorithm so `Y` will be the same size as `X`. And `nfft` denotes the number of `fft`.

Université Gustave Eiffel • Campus de Marne-la-Vallée
5, Boulevard Descartes • Champs-sur-Marne • 77454 Marne-la-Vallée CEDEX 2• France

We have done the Fast Fourier Transform of the all the hammer impacts of each testcase for all 5 beams.

4.4.1 First Beam (VL_R1FNTT_Vib-COBE_L_ent)

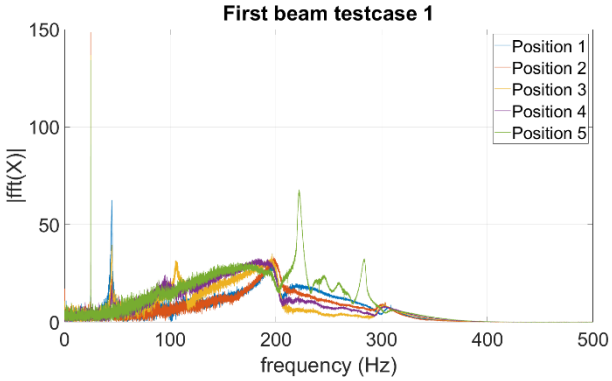

FIGURE 29 FREQUENCY ANALYSIS OF FIRST BEAM FOR ALL THE POSITION FOR TESTCASE 1

We can see in the Figure 29 highest peak is around 195 Hz. And as we don't have the time domain graph for testcase 2, hence we could not plot Fast Fourier Response (FFR).

4.4.2 Second Beam (VL_R1FNTT_Vib-COBE_L)

4.4.2.1 Second beam: Testcase 1

We have two hammer impacts of testcase 1, Figure 30 shows the first hammer impact and the second hammer impact can be found in the Appendix C.

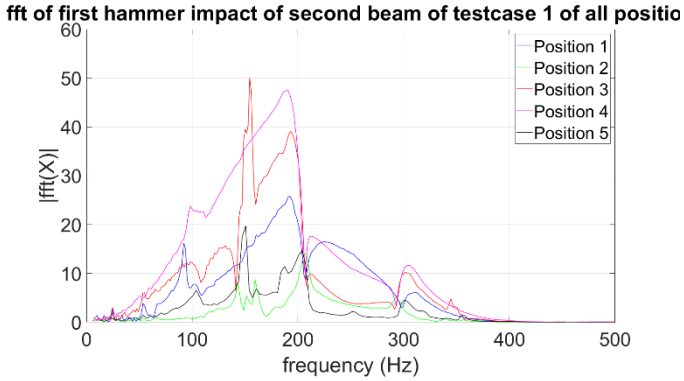

FIGURE 30 FREQUENCY ANALYSIS OF THE FIRST HAMMER IMPACT OF SECOND BEAM TESTCASE 1

In the Figure 30, we can find that the highest peak has the frequency of 190.56 Hz and the second highest is 305.305 Hz.

4.4.2.2 Second beam: Testcase 2

We have three hammer impacts of testcase 1, Figure 31 shows the first hammer impact and the second and third hammer impact can be found in the Appendix C.

Université Gustave Eiffel • Campus de Marne-la-Vallée
5, Boulevard Descartes • Champs-sur-Marne • 77454 Marne-la-Vallée CEDEX 2• France

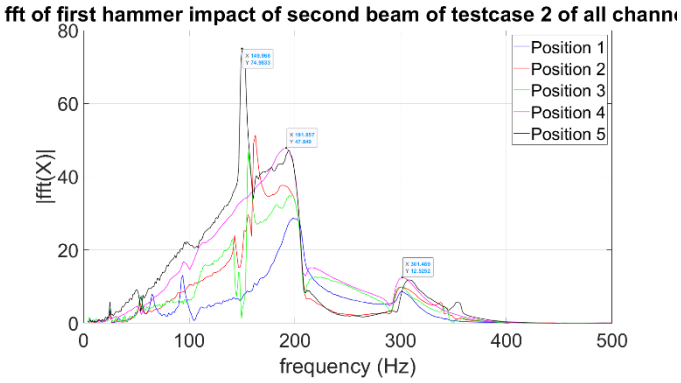

FIGURE 31 FREQUENCY ANALYSIS OF THE FIRST HAMMER IMPACT OF SECOND BEAM TESTCASE 2

We can see in the Figure 31, the highest peak has the frequency of 149.968 Hz, second highest is 191.85 Hz and the third highest is 301.489 Hz

4.4.3 Third beam (VL_R1F_Vib-COBE_L)

4.4.2.1 Third beam: Testcase 1

We have three hammer impacts of testcase 1, Figure 32 shows the first hammer impact and the second hammer impact can be found in the Appendix D.

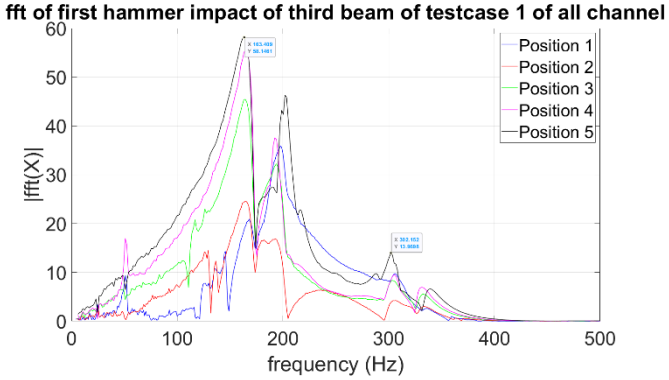

FIGURE 32 FREQUENCY ANALYSIS OF THE FIRST HAMMER IMPACT OF THIRD BEAM TESTCASE 1

We can see in the Figure 32, the highest peak has the frequency of 163.409 Hz, second highest is 201.94 Hz and the third highest is 302.152 Hz

4.4.2.2 Third beam: Testcase 2

We have three hammer impacts of testcase 1, Figure 33 shows the first hammer impact and the second hammer impact can be found in the Appendix D.

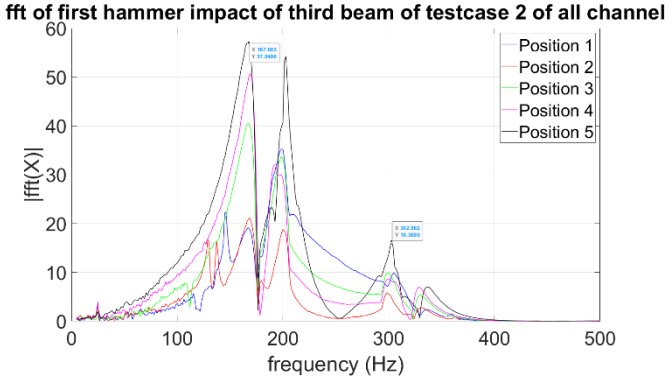

Université Gustave Eiffel • Campus de Marne-la-Vallée
5, Boulevard Descartes • Champs-sur-Marne • 77454 Marne-la-Vallée CEDEX 2• France

FIGURE 33 FREQUENCY ANALYSIS OF THE FIRST HAMMER IMPACT OF THIRD BEAM TESTCASE 2

We can see in the Figure 33, the highest peak has the frequency of 167.603 Hz, second highest is 202.888 Hz and the third highest is 302.869 Hz.

44.4 Fourth Beam (VN_R1F_NTT_VIB-COBE-VN)

4.4.4.1 Fourth beam: Testcase 1

We have three hammer impacts of testcase 1, Figure 34 shows the first hammer impact and the second and third hammer impact can be found in the Appendix E.

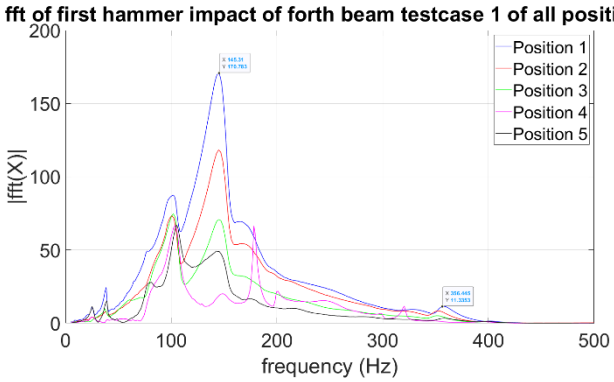

FIGURE 34 FREQUENCY ANALYSIS OF THE FIRST HAMMER IMPACT OF FOURTH BEAM TESTCASE 1

We can see in the Figure 34 the highest peak has the frequency of 145.31 Hz.

4.4.4.2 Fourth beam: Testcase 2

We have three hammer impacts of testcase 1, Figure 35 shows the first hammer impact and the second and third hammer impact can be found in the Appendix E.

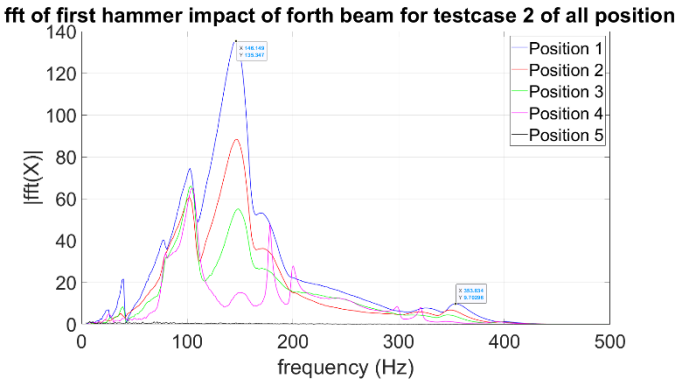

FIGURE 35 FREQUENCY ANALYSIS OF THE FIRST HAMMER IMPACT OF FOURTH BEAM TESTCASE 2

We can see in the Figure 35, the highest peak has the frequency of 146.149 Hz

4.4.5 Fifth beam (VN_R1F_VIB-COBE-VN)

4.4.5.1 Fifth beam: Testcase 1

We have three hammer impacts of testcase 1, Figure 36 shows the first hammer impact and the second and third hammer impact can be found in the Appendix F.

Université Gustave Eiffel • Campus de Marne-la-Vallée
5, Boulevard Descartes • Champs-sur-Marne • 77454 Marne-la-Vallée CEDEX 2• France

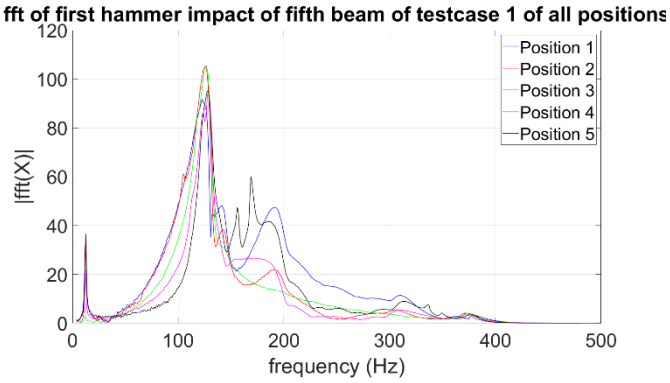

FIGURE 36 FREQUENCY ANALYSIS OF THE FIRST HAMMER IMPACT OF FIFTH BEAM TESTCASE 1

We can see in the Figure 36, the highest peak has the frequency of 126.472 Hz

4.4.5.2 Fifth beam: Testcase 2

We have three hammer impacts of testcase 1, Figure 37 shows the first hammer impact and the second and third hammer impact can be found in the Appendix F.

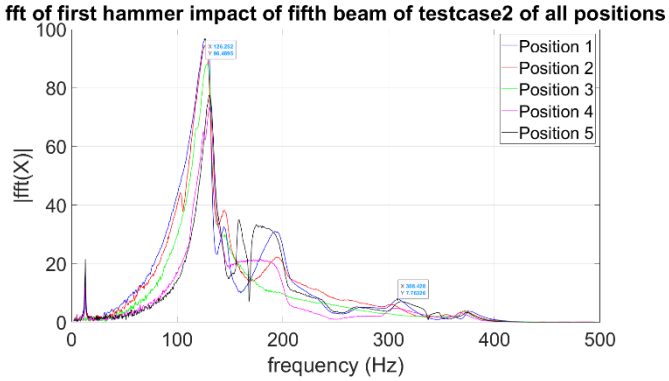

FIGURE 37 FREQUENCY ANALYSIS OF THE FIRST HAMMER IMPACT OF FIFTH BEAM TESTCASE 2

We can see in the Figure 37, the highest peak has the frequency of 126.25 Hz

4.5 Comparison with theoritical studies

4.5.1 Calculation of first natural frequency from the frequency graph

Considering the peaks of each hammer impact from the graph of the each testcase for every concrete beam, to calculate the first natural frequency by taking the average of them which is presented in Table 5 below:

Beams	Testcase	Hammer Impact	Frequency value from frequency domain graph (Hz)	Average of hammer impacts (Hz)	Average of testcases (Hz)
First beam VL_R1FNTT_Vib-COBE_L_ent	Testcase 1	First	195.00	195.00	195.00
Second beam VL_R1FNTT_Vib-COBE_L	Testcase 1	First	190.00	174.18	161.62
		Second	158.30		
	Testcase 2	First	149.96	149.08	
		Second	149.00		
		Third	148.30		
	Testcase 1	First	163.40	176.87	170.76

Université Gustave Eiffel • Campus de Marne-la-Vallée
5, Boulevard Descartes • Champs-sur-Marne • 77454 Marne-la-Vallée CEDEX 2• France

Third beam VL_R1F_Vib-COBE_L		Second	163.62		
		Third	203.57		
	Testcase 2	First	167.00	164.66	
		Second	163.00		
		Third	164.00		
Forth beam VN_R1F_NTT_VIB-COBE-VN	Testcase 1	First	145.31	142.96	143.46
		Second	143.06		
		Third	140.44		
	Testcase 2	First	146.15	143.99	
		Second	143.58		
		Third	142.26		
Fifth beam VN_R1F_VIB-COBE-VN	Testcase 1	First	126.47	124.64	123.34
		Second	127.65		
		Third	119.80		
	Testcase 2	First	125.41	122.04	
		Second	120.27		
		Third	120.44		

TABLE 5 CALCULATION FOR THE FREQUENCY FROM EXPERIMENTAL ANALYSIS

Hence, we can conclude the results in the following table:

Beam Names	1st natural frequency using EB theory f_{EB} (Hz)		1st natural frequency using TM theory f_{TB} (Hz)		Numerical f_{NR} (Hz)	Experimental f_{Ex} (Hz)
	L=0.8 m	L =1 m	L =0.8 m	L =1 m		
First beam VL_R1FNTT_Vib-COBE_L_ent	366.85	252.09	350.92	249.73	226.13	195.00
Second beam VL_R1FNTT_Vib-COBE_L	366.85	252.09	350.92	249.73	226.13	161.00
Third beam VL_R1F_Vib-COBE_L	348.26	223.62	333.51	221.87	214.68	170.00
Forth beam VN_R1F_NTT_VIB-COBE-VN	366.85	252.09	350.92	249.73	226.13	143.46
Fifth beam VN_R1F_VIB-COBE-VN	348.26	223.62	333.51	221.87	214.68	123.34

TABLE 6 EXPERIMENTAL RESULTS OF THE BEAMS

We see in the Table 6 that there is a difference in the value of frequency got from different theories and experimental study and Numerical study.

4.5.1.1 Comparison between the Theoretical results and Numerical results:

- The relative change percentage between the Euler Bernoulli theory result and Numerical result:

To calculate the relative change, we have used the formula:

$$\left|\frac{f_{NR}-f_{EB}}{f_{EB}} \times 100\right| = \text{relative change percentage} \qquad \text{(Eq.32)}$$

Université Gustave Eiffel • Campus de Marne-la-Vallée
5, Boulevard Descartes • Champs-sur-Marne • 77454 Marne-la-Vallée CEDEX 2• France

Beams	L =1 m
First beam VL_R1FNTT_Vib-COBE_L_ent	10.29%
Second beam VL_R1FNTT_Vib-COBE_L	10.29%
Third beam VL_R1F_Vib-COBE_L	4.02%
Forth beam VN_R1F_NTT_VIB-COBE-VN	10.29%
Fifth beam VN_R1F_VIB-COBE-VN	4.02%

TABLE 7 THE RELATIVE CHANGE BETWEEN THE EULER BERNOULLI THEORY RESULT AND NUMERICAL RESULT

In Table 7, we can see that Euler Bernoulli theory has the correspondence with the Numerical result.

- The relative change percentage between the Timoshenko theory result and Numerical result:

To calculate the relative change, we have used the formula:

$$\left|\frac{f_{NR}-f_{TB}}{f_{TB}} \times 100\right| = \text{relative change percentage} \qquad \text{(Eq.33)}$$

Beams	L =1 m
First beam VL_R1FNTT_Vib-COBE_L_ent	9.23%
Second beam VL_R1FNTT_Vib-COBE_L	9.23%
Third beam VL_R1F_Vib-COBE_L	3.16%
Forth beam VN_R1F_NTT_VIB-COBE-VN	9.23%
Fifth beam VN_R1F_VIB-COBE-VN	3.16%

TABLE 8 THE RELATIVE CHANGE BETWEEN THE EULER BERNOULLI THEORY RESULT AND NUMERICAL RESULT

In the Table 8, we find that the Timoshenko result converges more than the Euler Bernoulli theory towards the Numerical Result, which validate the link between the Timoshenko theory and Numerical analysis. This also proves that the Timoshenko beam theory gives more accuracy.

4.5.1.2 Comparison between the Theoretical results and Experimental results:

- The relative change percentage between the Euler Bernoulli theory result and Timoshenko theory result:

To calculate the relative change, we have used the formula:

$$\left|\frac{f_{TB}-f_{EB}}{f_{EB}} \times 100\right| = \text{relative change percentage} \qquad \text{(Eq.33)}$$

where,

f_{EB} is the frequency using Euler Bernoulli beam theory;

f_{TB} is the frequency using Timoshenko beam theory.

Beams	L=0.8 m	L =1 m
First beam VL_R1FNTT_Vib-COBE_L_ent	4.34%	0.93%
Second beam VL_R1FNTT_Vib-COBE_L	4.34%	0.93%
Third beam VL_R1F_Vib-COBE_L	4.23%	0.78%
Forth beam VN_R1F_NTT_VIB-COBE-VN	4.34%	0.93%
Fifth beam VN_R1F_VIB-COBE-VN	4.23%	0.78%

Université Gustave Eiffel • Campus de Marne-la-Vallée
5, Boulevard Descartes • Champs-sur-Marne • 77454 Marne-la-Vallée CEDEX 2• France

TABLE 9 THE RELATIVE CHANGE BETWEEN THE EULER BERNOULLI THEORY RESULT AND TIMOSHENKO THEORY RESULT

We can see from the Table 9, that for short length ($L = 0.8\ m$) Timoshenko theory gives more precise result than Euler Bernoulli theory.

- The relative change between the Euler Bernoulli theory result and the Experimental result is as follows:

Here the formula that we have used is:

$$\left|\frac{f_{Ex}-f_{EB}}{f_{EB}} \times 100\right| = \text{relative change percentage} \quad \text{(Eq.34)}$$

where,

f_{Ex} is the frequency using the Experimental result

Beams	L=0.8 m	L =1 m
First beam VL_R1FNTT_Vib-COBE_L_ent	46.84%	22.64%
Second beam VL_R1FNTT_Vib-COBE_L	56.11%	36.13%
Third beam VL_R1F_Vib-COBE_L	51.18%	23.97%
Forth beam VN_R1F_NTT_VIB-COBE-VN	60.89%	43.1%
Fifth beam VN_R1F_VIB-COBE-VN	64.58%	44.8%

TABLE 10 THE RELATIVE CHANGE BETWEEN EULER BERNOULLI THEORY RESULT AND EXPERIMENTAL RESULT

From Table 10, we see that for L=0.8 m , Euler Bernoulli results deviate significantly from the experimental results where in for L=1 m, the deviation seems lesser.

- The relative change between Timoshenko theory result and Experimental result is as follows:

Here, we used the formula:

$$\left|\frac{f_{Ex}-f_{TB}}{f_{TB}} \times 100\right| = \text{ relative change percentage} \quad \text{(Eq.35)}$$

Beams	L=0.8 m	L =1 m
First beam VL_R1FNTT_Vib-COBE_L_ent	44.43%	21.9%
Second beam VL_R1FNTT_Vib-COBE_L	53.81%	35.53%
Third beam VL_R1F_Vib-COBE_L	49.02%	23.37%
Forth beam VN_R1F_NTT_VIB-COBE-VN	59.11%	42.55%
Fifth beam VN_R1F_VIB-COBE-VN	63.01%	44.40%

TABLE 11 THE RELATIVE CHANGE BETWEEN TIMOSHENKO THEORY RESULT AND EXPERIMENTAL RESULT

We can observe from the Table 11, that there is still significant difference between the Timoshenko beam theory result and the experimental result but if we compare with the Table 10, Euler Bernoulli shows more divergence from the experimental value.

Université Gustave Eiffel • Campus de Marne-la-Vallée
5, Boulevard Descartes • Champs-sur-Marne • 77454 Marne-la-Vallée CEDEX 2• France

5 Conclusions and Results and Discussions

The angular frequency (ω) depends on the young's modulus of the beam, moment of inertia of the beam, mass density and cross section area of the beam.

And when the density was calculated in July 2023 it was,

$$\rho_1 = 2416\ kg.m^{-3} \quad \text{(Eq.36)}$$

For the mass density of the beam in June 2024, we measured the following:

Mass of the beam with the two supports = 38.2 kg;

Mass of the two supports = 0.193 kg;

Therefore, the mass of the beam comes out to be,

$38.2 - 0.193 = 38.007\ kg$

Volume of the beam = $(0.125 \times 0.125 \times 1)\ m^3$

The density of the beam, $\rho = \frac{mass\ of\ the\ beam}{volume\ of\ the\ beam}$

$$\rho_2 = \frac{38.007}{0.125 \times 0.125 \times 1}$$

$$\rho_2 = 2432.44\ kg.m^{-3} \quad \text{(Eq.37)}$$

The relative change in the densities from the Eq.36 and Eq.37, it is 0.6%, which is even less than 1% so we can neglect the density effect in the natural frequency.

There is a little change in the moment of inertia due to the DEF, which can be neglected too. The cross-sectional area also remains the same, therefore the only factor which can affect the natural frequency of the beam is the young's modulus.

The relation between the young's modulus and natural frequency is the directly proportional. As there is a decrease in the value of young's modulus throughout the process so there is also a decrement in the natural frequency of the beam.

The theoretical and the Numerical Analysis are similar which represented by the small relative difference; however, we see a significant difference between the experimental results and theoretical/numerical results for the first natural frequency of the beam. This could be explained by the parameters are used in the models are not the same as experiment. Additionally, it should be noted that the geometrical parameters are changed with smaller value after several months because of the chemical phenomenon inside the concrete beams.

Université Gustave Eiffel • Campus de Marne-la-Vallée
5, Boulevard Descartes • Champs-sur-Marne • 77454 Marne-la-Vallée CEDEX 2• France

6 Personal skill Development

In this research internship, I had the invaluable opportunity to refine and enhance a multitude of skills and competencies. I developed both professionally as well as personally. I honed my MATLAB skills, mastering advanced functionalities that elevated the quality of my analytical work. This internship provided a unique chance to work at the intersection of mechanical and civil engineering, fostering a deeper understanding of interdisciplinary collaboration and problem-solving. Being a mechanical student some concepts I knew before because of which it was easier for me to understand the research related topics. I performed some of the experimentation work with the research team, which gave me an idea of how things work.

Additionally, I became proficient in using Microsoft Word and PowerPoint, which allowed me to create professional documents and compelling presentations. I also got a chance to deliver my work in the form of presentation which made me bold to speak out publicly. One of the very interesting things that I learnt is the Numerical simulation Finite Element Analysis, which was actually a brainstorming. I did fail many times but eventually I was able to get the correct result. This actually made me learn the fact, “no matter how many times you fail, you should always be ready to get up again and fight for it”. And I finally finished my research work and validated by the supervisors.

At the end of internship, I also submitted a report corresponding to the research study which enhanced my writing skills and enabled me to articulate complex ideas and research findings with clarity and precision.

Apart from this, I was fortunate to have lab mates very humble and polite towards me and they always helped me understand rules and regulation and provided me every possible information for my stay in France.

Beyond technical and academic growth, my internship immersed me in the rich and vibrant French culture, broadening my cultural perspective and enriching my personal development. I learned to appreciate the nuances of French social norms, traditions, and etiquette, which was both enlightening and rewarding. People here are very supportive to others and always ready to serve. The blend of technical training, interdisciplinary exposure, and cultural immersion made this experience incredibly fulfilling, leaving me with a wealth of knowledge and a profound sense of accomplishment.

Université Gustave Eiffel • Campus de Marne-la-Vallée
5, Boulevard Descartes • Champs-sur-Marne • 77454 Marne-la-Vallée CEDEX 2• France

7 References

[1] https://learnaboutstructures.com/Bernoulli-Euler-Beam-Theory.

[2] https://encyclopedia.pub/entry/34559

[3] https://www.researchgate.net/figure/The-free-body-diagram-of-Timoshenko-beam-element_fig1_266268378

[4] https://support.sw.siemens.com/en-US/okba/KB000036272_EN_US/Natural-Frequency-and-Resonance/index.html

Université Gustave Eiffel • Campus de Marne-la-Vallée
5, Boulevard Descartes • Champs-sur-Marne • 77454 Marne-la-Vallée CEDEX 2• France

8 Appendix

Appendix A- Program MATLAB for FEM

Here is the MATLAB code for FEM done for the beam:

```
close all;
clear all;

% Create a structural modal model
smodel = createpde('structural', 'modal-solid');

% Import the geometry from the STL file
importGeometry(smodel,'concrete v0.stl');
% Plot the geometry with face labels
figure;
set(gca, 'FontSize', 20)
pdegplot(smodel, 'FaceLabels', 'on','EdgeLabels','on');
title('Geometry with Face Labels and Edge labels');

% Generate the mesh
msh = generateMesh(smodel); % Adjust Hmax as needed for finer mesh

% Plot the mesh
figure;
set(gca, 'FontSize', 20)
pdeplot3D(smodel);
title('Generated Mesh');

% Define the material properties
structuralProperties(smodel, 'YoungsModulus', 41.4e9, 'PoissonsRatio', 0.19,
'MassDensity', 2416);
% Apply fixed boundary conditions to the edges near x = 0.1 m and x = 0.9 m
structuralBC(smodel, 'Edge', 6, 'ZDisplacement', 0);
structuralBC(smodel, 'Edge', 11, 'ZDisplacement', 0);

% Solve the model for the specified frequency range
modalResults = solve(smodel, 'FrequencyRange', [1, 15000]);

% Extract and display the first 5 natural frequencies
naturalFrequencies = modalResults.NaturalFrequencies/(2*pi);
disp('First 6 Natural Frequencies (Hz):');
disp(naturalFrequencies(1:6));

% Visualize the first 5 mode shapes
figure;
for i = 1:6
    subplot(3, 2, i);
    pdeplot3D(smodel, 'ColorMapData', modalResults.ModeShapes.uz(:,i));
    set(gca, 'FontSize', 20)
    title(['Mode Shape ', num2str(i), ' at Frequency ',
num2str(naturalFrequencies(i)), ' Hz']);
end
```

Appendix B- Program MATLAB for frequency analysis

Let's see an example of the script of the MATLAB code, the followed code is to aligned the time domain graph for the testcase 1 for fifth beam as there was a time delay in the signal with one another.

Université Gustave Eiffel • Campus de Marne-la-Vallée
5, Boulevard Descartes • Champs-sur-Marne • 77454 Marne-la-Vallée CEDEX 2• France

Beam	File name
First Beam	20230728_vibrations_poutresVN_R1F_VIB-COBE-VN_S1_29278.csv
Second Beam	20230728_vibrations_poutresVN_R1F_VIB-COBE-VN_S1_29279.csv
Third Beam	20230728_vibrations_poutresVN_R1F_VIB-COBE-VN_S1_29280.csv
Fourth Beam	20230728_vibrations_poutresVN_R1F_VIB-COBE-VN_S1_40197.csv
Fifth Beam	20230728_vibrations_poutresVN_R1F_VIB-COBE-VN_S1_40202.csv

```
%%fifth beam test case 1
clear all
close all
%% Import 1st channel
opts = delimitedTextImportOptions("NumVariables", 2);
opts.DataLines = [21, Inf];
opts.Delimiter = ",";
opts.VariableNames = ["Var1", "ch3"];
opts.SelectedVariableNames = "ch3";
opts.VariableTypes = ["string", "double"];
opts.ExtraColumnsRule = "ignore";
opts.EmptyLineRule = "read";
opts = setvaropts(opts, "Var1", "WhitespaceRule", "preserve");
opts = setvaropts(opts, "Var1", "EmptyFieldRule", "auto");
position1 = readtable("File name", opts);
clear opts

%%
Fs = 4096;                      %% sampling frequency
nfft = 4096*16;                  %% number of fft
fre = (0:nfft/2-1)*Fs/nfft;            %% frequency
dt = 1/Fs;

ch1 = position1;
ch1 = table2array(ch1);
ch1 = ch1-mean(ch1(1:100));
time_ch1 = transpose(linspace(0, dt*(length(ch1)-1), length(ch1)));
fft_signal1 = fft(ch1, nfft);
fft_signal1 = fft_signal1(1:nfft/2);

ch2 = position2;
ch2 = table2array(ch2);
ch2 = ch2-mean(ch2(1:100));
time_ch2 = transpose(linspace(0, dt*(length(ch2)-1), length(ch2)));

ch3 = position3;
ch3 = table2array(ch3);
ch3 = ch3-mean(ch3(1:100));
time_ch3 = transpose(linspace(0, dt*(length(ch3)-1), length(ch3)));

ch4 = position4;
ch4 = table2array(ch4);
ch4 = ch4-mean(ch4(1:100));
time_ch4 = transpose(linspace(0, dt*(length(ch4)-1), length(ch4)));

ch5 = position5;
ch5 = table2array(ch5);
ch5 = ch5-mean(ch5(1:100));
time_ch5 = transpose(linspace(0, dt*(length(ch5)-1), length(ch5)));

figure(1)
```


Université Gustave Eiffel • Campus de Marne-la-Vallée
5, Boulevard Descartes • Champs-sur-Marne • 77454 Marne-la-Vallée CEDEX 2• France

```
hold on
plot(ch1)
plot(ch2)
plot(ch3)
plot(ch4)
plot(ch5)

diff_pos5 = 40954-34843;
ch5(1:diff_pos5) = [];
time_ch5(1:diff_pos5) = [];
time_ch5 = time_ch5 - time_ch5(1);

diff_pos4 = 36896-34843;
ch4(1:diff_pos4) = [];
time_ch4(1:diff_pos4) = [];
time_ch4 = time_ch4 - time_ch4(1);

diff_pos2 = 34908-34843;
ch2(1:diff_pos2) = [];
time_ch2(1:diff_pos2) = [];
time_ch2 = time_ch2 - time_ch2(1);

diff_pos1 = 38924-34843;
ch1(1:diff_pos1) = [];
time_ch1(1:diff_pos1) = [];
time_ch1 = time_ch1 - time_ch1(1);

figure(2)
hold on
plot(time_ch1, ch1, 'linewidth', 1.5)
plot(time_ch2, ch2, 'linewidth', 1.5)
plot(time_ch3, ch3, 'linewidth', 1.5)
plot(time_ch4, ch4, 'linewidth', 1.5)
plot(time_ch5, ch5, 'linewidth', 1.5)
box on
grid on
xlim([8 13])
set(gca, 'FontSize', 20)
xlabel('Time (s)')
ylabel('Acceleration (m/s^2)')
legend('Position 1', 'Position 2', 'Position 3', 'Position 4', 'Position 5',
'location', 'Southeast')
%
figure(3)
hold on
plot(time_ch1, ch1, 'linewidth', 1.5)
plot(time_ch2, ch2, 'linewidth', 1.5)
plot(time_ch3, ch3, 'linewidth', 1.5)
plot(time_ch4, ch4, 'linewidth', 1.5)
plot(time_ch5, ch5, 'linewidth', 1.5)
box on
grid on
xlim([8.45 8.9])
set(gca, 'FontSize', 20)
xlabel('Time (s)')
ylabel('Acceleration (m/s^2)')
legend('Position 1', 'Position 2', 'Position 3', 'Position 4', 'Position 5',
'location', 'Southeast')
```

Appendix C- Graphics of FFR of VL_R1FNTT_Vib-COBE_L

Second Beam- Testcase 1

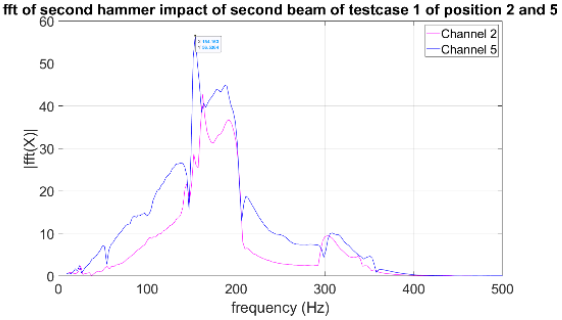

FIGURE 38 SECOND HAMMER IMPACT OF SECOND BEAM FOR TESTCASE 1

Second Beam- Testcase 2

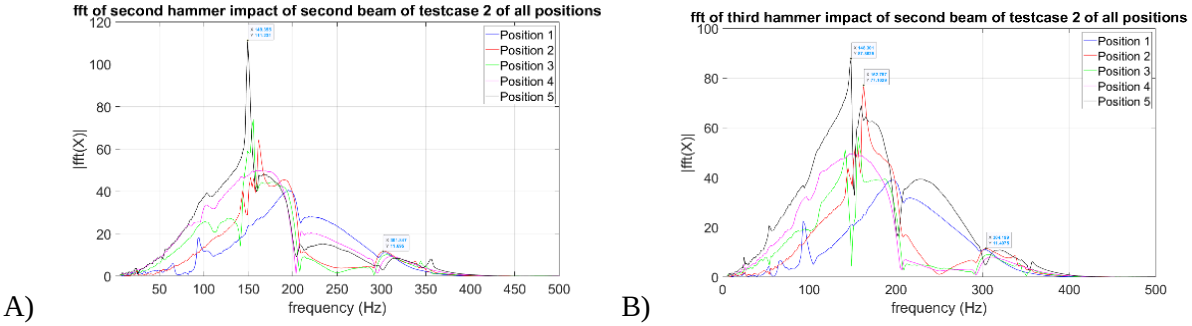

A) B)

FIGURE 39 A) SECOND HAMMER IMPACT B) THIRD HAMMER IMPACT OF SECOND BEAM FOR TESTCASE 2

Appendix D- Graphics of FFR of VL_R1F_Vib-COBE_L

Third Beam- Testcase 1

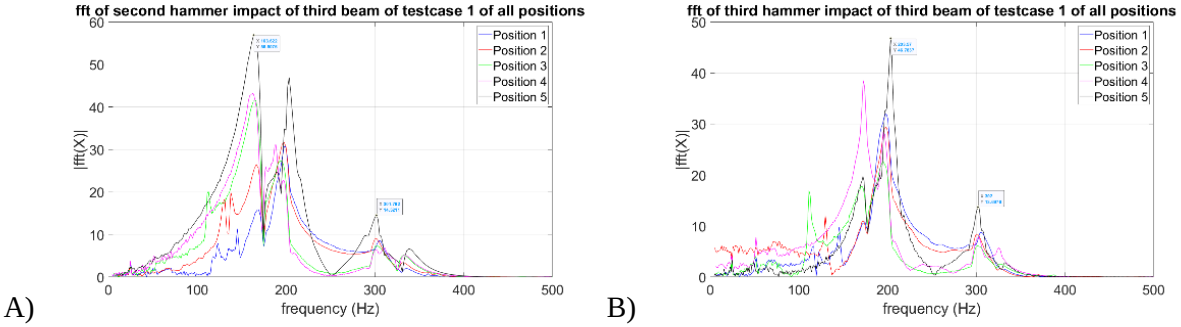

A) B)

FIGURE 40 A) SECOND HAMMER IMPACT B) THIRD HAMMER IMPACT OF THIRD BEAM FOR TESTCASE 1

Third Beam- Testcase 2

Université Gustave Eiffel • Campus de Marne-la-Vallée
5, Boulevard Descartes • Champs-sur-Marne • 77454 Marne-la-Vallée CEDEX 2• France

A)

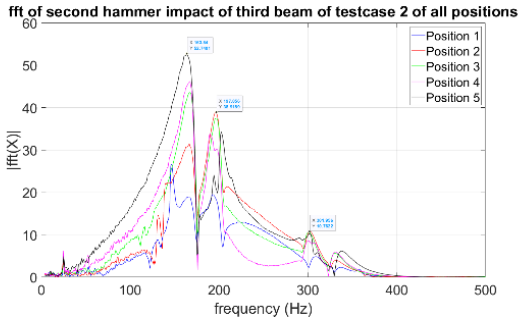

B)

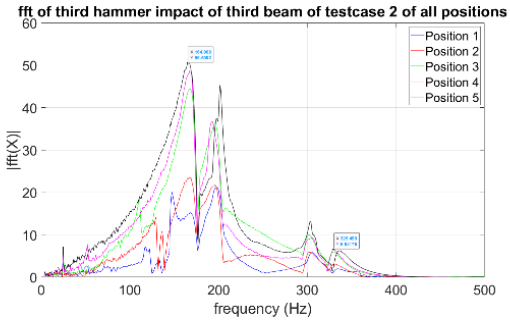

FIGURE 41 A) SECOND HAMMER IMPACT B) THIRD HAMMER IMPACT OF THIRD BEAM FOR TESTCASE 2

Appendix E- Graphics of FFR of VN_R1F_NTT_VIB-COBE-VN

Fourth Beam- Testcase 1

A)

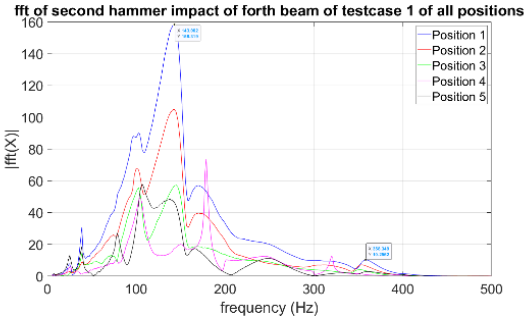

B)

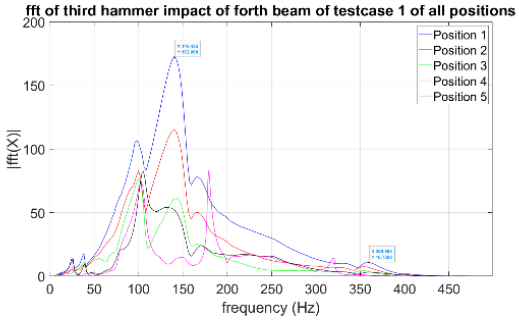

FIGURE 42 A) SECOND HAMMER IMPACT B) THIRD HAMMER IMPACT OF FOURTH BEAM FOR TESTCASE 1

Fourth Beam- Testcase 2

A)

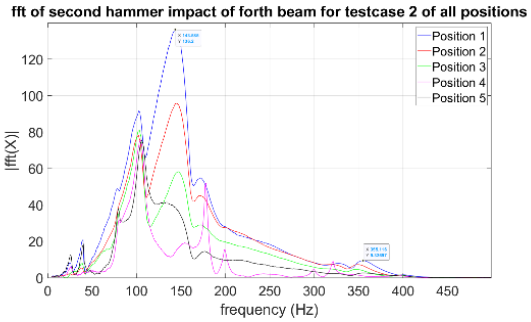

B)

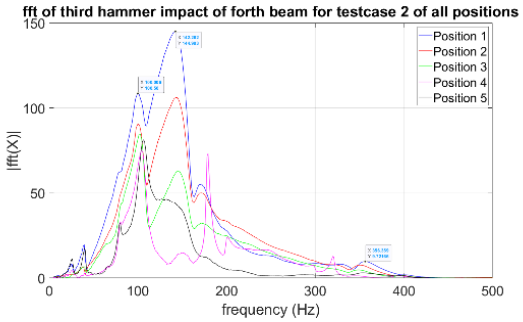

FIGURE 43 A) SECOND HAMMER IMPACT B) THIRD HAMMER IMPACT OF FOURTH BEAM FOR TESTCASE 2

Appendix F- Graphics of FFR of VN_R1F_VIB-COBE-VN

Fifth Beam- Testcase 1

Université Gustave Eiffel • Campus de Marne-la-Vallée
5, Boulevard Descartes • Champs-sur-Marne • 77454 Marne-la-Vallée CEDEX 2• France

A)

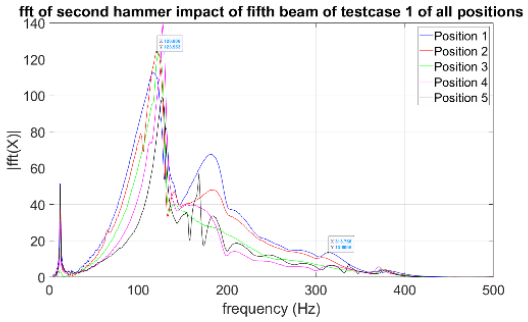

B)

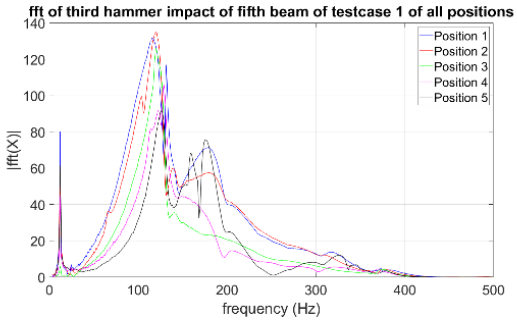

FIGURE 44 A) SECOND HAMMER IMPACT B) THIRD HAMMER IMPACT OF FIFTH BEAM FOR TESTCASE 1

Fifth Beam- Testcase 2

A)

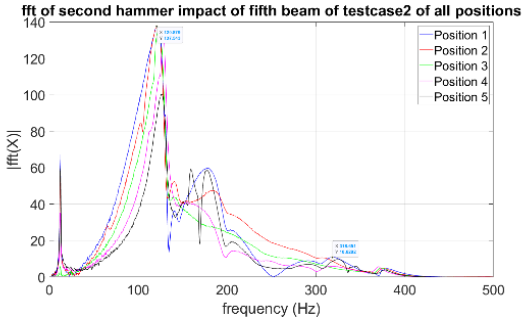

B)

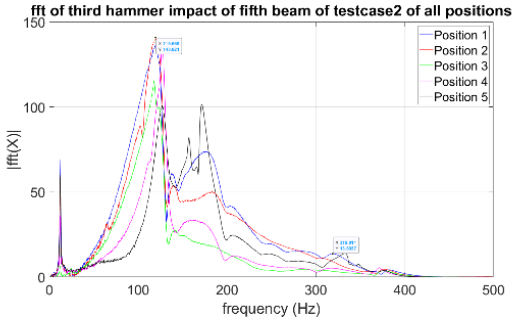

FIGURE 45 A) SECOND HAMMER IMPACT B) THIRD HAMMER IMPACT OF FIFTH BEAM FOR TESTCASE 2

Université Gustave Eiffel • Campus de Marne-la-Vallée
5, Boulevard Descartes • Champs-sur-Marne • 77454 Marne-la-Vallée CEDEX 2• France

Appendix G- Records of all impacts of JULY 2023 experimentation

Month of Experimentation	Beam	Test	Detail	Sensors positions	
July, 2023	1st beam VL_R1FNTT_Vib-COBE_L_ent	1st test	**Only one impact**	1st 2nd 3rd 4th 5th	**20278** **20279** **20280** **40197** **40202**
		2nd test	**The signal that we stored do not give the desired result for the test 2.**		
	2nd beam VL_R1FNTT_Vib-COBE_L	1st test	**We have 2 impacts**	1st 2nd 3rd 4th 5th	**20278** **20279** **20280** **40197** **40202**
		2nd test	**We have 3 impacts**		
	3rd beam VL_R1F_Vib-COBE_L	1st test	**We have 3 impacts**	1st 2nd 3rd 4th 5th	**20278** **20279** **20280** **40197** **40202**
		2nd test	**We have 3 impacts**		
	4th beam VN_R1F_NTT_VIB-COBE-VN	1st test	**We have 3 impacts**	1st 2nd 3rd 4th 5th	**20278** **20279** **20280** **40197** **40202**
		2nd test	**We have 3 impacts**		
	5th beam VN_R1F_VIB-COBE-VN	1st test	**We have 3 impacts**	1st 2nd 3rd 4th 5th	**20278** **20279** **20280** **40197** **40202**
		2nd test	**We have 3 impacts**		